JACS
JOURNAL OF THE AMERICAN CHEMICAL SOCIETY
pubs.acs.org/JACS
Article

Real-Time High-Sensitivity Reaction Monitoring of Important Nitrogen-Cycle Synthons by ^{15}N Hyperpolarized Nuclear Magnetic Resonance

Peter J. Rayner, Marianna Fekete, Callum A. Gater, Fadi Ahwal, Norman Turner, Aneurin J. Kennerley, and Simon B. Duckett*

Cite This: *J. Am. Chem. Soc.* 2022, 144, 8756–8769
Read Online
ACCESS | Metrics & More | Article Recommendations | Supporting Information

ABSTRACT: Here, we show how signal amplification by reversible exchange hyperpolarization of a range of ^{15}N-containing synthons can be used to enable studies of their reactivity by ^{15}N nuclear magnetic resonance (NO_2^- (28% polarization), ND_3 (3%), $PhCH_2NH_2$ (5%), NaN_3 (3%), and NO_3^- (0.1%)). A range of iridium-based spin-polarization transfer catalysts are used, which for NO_2^- work optimally as an amino-derived carbene-containing complex with a DMAP-d_2 coligand. We harness long ^{15}N spin-order lifetimes to probe in situ reactivity out to $3 \times T_1$. In the case of NO_2^- (T_1 17.7 s at 9.4 T), we monitor $PhNH_2$ diazotization in acidic solution. The resulting diazonium salt (^{15}N-T_1 38 s) forms within 30 s, and its subsequent reaction with NaN_3 leads to the detection of hyperpolarized PhN_3 (T_1 192 s) in a second step via the formation of an identified cyclic pentazole intermediate. The role of PhN_3 and NaN_3 in copper-free click chemistry is exemplified for hyperpolarized triazole (T_1 < 10 s) formation when they react with a strained alkyne. We also demonstrate simple routes to hyperpolarized N_2 in addition to showing how utilization of ^{15}N-polarized $PhCH_2NH_2$ enables the probing of amidation, sulfonamidation, and imine formation. Hyperpolarized ND_3 is used to probe imine and ND_4^+ (T_1 33.6 s) formation. Furthermore, for NO_2^-, we also demonstrate how the ^{15}N-magnetic resonance imaging monitoring of biphasic catalysis confirms the successful preparation of an aqueous bolus of hyperpolarized $^{15}NO_2^-$ in seconds with 8% polarization. Hence, we create a versatile tool to probe organic transformations that has significant relevance for the synthesis of future hyperpolarized pharmaceuticals.

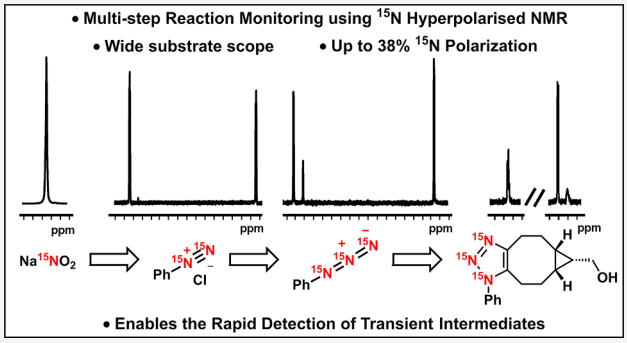

INTRODUCTION

Positron emission tomography (PET) is a very sensitive technique that uses gamma cameras to image changes in metabolic processes, blood flow, and agent absorption in the body. It takes long-lived radionuclides generated using a cyclotron that are then embedded into a suitable receptor to create the radiopharmaceuticals that convey the diagnostic response. Unfortunately, this process can be complex and costly. Magnetic resonance imaging (MRI) is another powerful diagnostic method, but inherent low sensitivity means that routine clinical measurements probe highly abundant water.

Consequently, there has been a great deal of excitement in the clinical community with a method called hyperpolarization that gives MRI the sensitivity needed to visualize changes in metabolic flux by detecting biomolecules that encode disease. The most clinically developed method currently involves the use of dissolution dynamic nuclear polarization (d-DNP).[1−3] One alternative method to create hyperpolarization is *para*hydrogen (p-H_2)-induced polarization (PHIP), which despite being discovered in the 1980s is only now receiving worldwide attention. Three recent significant PHIP advances that utilize p-H_2 are signal amplification by reversible exchange (SABRE),[4] p-H_2-induced polarization with side-arm hydrolysis,[5] and the rapid hyperpolarization and purification of the metabolite fumarate.[6,7] As p-H_2 can be prepared to a level of 50% purity by simply cooling H_2 gas by liquid nitrogen,[8] one could imagine the widespread future use of this MR sensitization approach.

Here, we demonstrate how it is possible to turn PHIP into a versatile tool for the in situ synthesis of a family of long-lived and highly MR visible precursors containing ^{15}N, akin to the radionuclides of PET. These reactive intermediates are rapidly embedded into important molecular reporters to illustrate the creation of the hyperpharmaceutical. We achieve this by harnessing reactive species like nitrite (NO_2^-), nitrosonium

Received: March 9, 2022
Published: May 4, 2022

https://doi.org/10.1021/jacs.2c02619
J. Am. Chem. Soc. 2022, 144, 8756–8769

(NO^+), and ammonia (NH_3), representing simple building blocks which can be transformed into a wide range of hyperpolarized materials.

Our method takes their ^{15}N isotopologues and uses PHIP to first hyperpolarize them. Thus we create an imbalance in one of the ^{15}N's two possible nuclear spin orientations (+1/2 or −1/2) which can potentially be maintained for 10's of minutes if stored in an appropriate magnetic field.[9−11] We focus on establishing this concept by reference to nuclear magnetic resonance (NMR), a technique that is used by many scientific disciplines. NMR mainly detects ^1H responses, because the most commonly probed alternative nucleus, ^{13}C, is 6400 times harder to detect than ^1H. This is due to ^{13}C's 1% abundance and small gyromagnetic ratio (γ). Consequently, the Zeeman splitting yielding the resonance frequency is four times smaller than ^1H, and a minute macroscopic nuclear magnetization occurs, which is detected by NMR.

Less utilized ^{15}N has a highly informative 1350 ppm chemical shift range and long T_1,[9] but as ^{15}N is only 0.36% abundant and has a γ 10 times smaller than ^1H, it is 260,000 times harder to detect. Hence, high-concentration samples and extensive signal averaging are needed for NMR studies at natural abundance. Despite this limitation, nitrite ions have been probed by ^{15}N NMR in solution and the solid state[12] and used to study chemodenitrification in humic substances[13] and nitric oxide release from copper sites, so its utility is established.[14] Importantly, the ^{15}N isotope can be sourced cheaply in materials like $^{15}NH_4Cl$ and $Na^{15}NO_2$, and this offers routes to synthesize other isotopically labeled compounds such as pharmaceuticals. Hyperpolarized $Na^{15}NO_2$, created by *d*-DNP, has been studied.[15]

The sensitivity gains provided by PHIP have already been used widely to aid the study of organic and inorganic chemicals, and it has made the detection of previously hidden intermediates possible.[16−19] Our aim here is to illustrate the hyper-pharmaceutical concept while establishing that we can track chemical reactivity, complete the diagnostic fingerprinting of materials, and dramatically expand chemical diversity in the field of hyperpolarization.

We start with nitrite (NO_2^-), a reagent that is formed during the nitrification of ammonia by nitrosomas within the nitrogen cycle.[20] While mammals do not absorb nitrites directly, plants use it to form essential nitrogen-containing molecules such as amino acids and further aerobic oxidation of nitrite leads to nitrate. Nitrite is used as a food additive for cured meats[21] and approximately 7% of our ingested nitrite comes this source, while the remainder comes from the enterosalivary pathway.[3,22] While nitrites are noncarcinogenic, their ability to form nitrosamines can lead to toxicity[23] as examined by the research community and mainstream media.[24,25] The action of methmyogolbin production by nitrite is, however, beneficial in the treatment of cyanide poisoning and sodium nitrite remains as one of the primary antidotes for acute intoxication.[26]

The nitrite ion, usually as sodium nitrite, finds widespread use in the chemical industry, because of its oxidizing properties and role in organic transformations; common examples are the Sandmeyer reaction, which transforms aryl amines into aryl halides, and the diazotization reaction that is used en route to the formation of dyes and pigments.[27]

Nitrite is also an ambidentate ligand that can bind to metals via the N- or O-atoms to form nitro or nitrito complexes, respectively,[28,29] with Ni[30−33] and Pt[34−36] examples being the most prevalent. As the PHIP hyperpolarization method SABRE works through reversible binding of the agent that is set to become hyperpolarized to a metal complex, we hypothesized that polarization of NO_2^- via such a route is possible.[4,11,37,38]

In fact, there are a few examples of ionic species such as sodium pyruvate,[39,40] sodium acetate,[41] and naicin[42] that undergo SABRE. This method requires the creation of a scalar coupling network between the target agent and *p*-H_2-derived protons in a catalyst.[43−46] Hence, an η^1-NO_2 (*N*-nitro) complex with a potentially large hydride-^{15}N coupling would be preferred over η^1-ONO (*O*-nitrito) or η^2-O−N−O (*O*,*O*-bidentate) linkage isomers. Theoretical descriptions of SABRE are provided by Barskiy and others[43,44,47] and account for the magnetization transfer conditions needed to sensitize a range of agents.[45] Transfer is optimized at low magnetic fields, typically 6 mT for ^1H, or through *r.f.* excitation at high field.[48] When combined with suitable catalyst lifetimes, this has driven the efficient sensitization of ^1H, ^{13}C, ^{15}N, ^{19}F, ^{31}P, and ^{29}Si (etc.)[39−41,49−59] nuclei.

Here, we also evaluate the azide anion, an excellent nucleophile that readily forms organic azides such as the antiretroviral AZT, Avapro, Diova, and Tamiflu. This functionality can be readily reduced to create amines, and through the Curtius rearrangement carbamates. Copper-catalyzed azide-alkyne cycloadditions or click reactions are also important. Consequently, azide represents an important precursor to agrochemicals, pharmaceuticals, and natural products so its successful hyperpolarization is also desirable.

Typically, when an iridium *N*-heterocyclic carbene (NHC) catalyst is used, products can be created whose NMR signal strengths are many orders of magnitude higher than those which would be obtained at thermal equilibrium.[60,61] Warren et al. in particular stand-out for their work on $^{15}N^{68}$ in a refinement called SABRE-SHEATH,[51,56] and up to 79% ^{15}N polarization has recently been reported for a range of neutral Lewis bases.[62] Several alternative radio-frequency transfer strategies have also been exemplified,[48,63,64] and given one of the goals of SABRE is in vivo detection, water-soluble SABRE catalysts have been described,[65,66] with the in vitro MRI detection of an ^{15}N response already illustrated.[66] Tessari et al. have developed a number of analytical science applications for SABRE[67] and other catalyst types have been reported.[68] Furthermore, hyperpolarized long-lived singlet states, as pioneered by Levitt,[69] have been created and detected after their formation.[50,70−74] Consequently, we might expect the benefits of such a simple approach to sensitize a range of ^{15}N-containing reagents to be substantial.

RESULTS AND DISCUSSION

Demonstration That an Active SABRE Catalyst Forms with $Na^{15}NO_2$. As indicated, for successful SABRE transfer to occur, the formation of a complex exhibiting spin−spin couplings between the bound substrate and *p*-H_2-derived hydride nuclei is required. Classically, this involves the reaction of a precatalyst (most commonly [IrCl(COD)(IMes)] (**1**) (IMes = 1,3-bis(2,4,6-trimethylphenyl)imidazolylidene)), with an excess of the selected substrate under a H_2 atmosphere. Complexes of type $[Ir(H)_2(IMes)(sub)_3]Cl$, when the substrate is a neutral *N*-heterocycle such as pyridine, meet this requirement.[4] Consequently, our initial efforts targeted the synthesis of an active SABRE catalyst with bound NO_2^- rather than pyridine.

When $Na^{15}NO_2$ (1 equiv) was added to a solution of [IrCl(COD)(IMes)] (**1**, 5 mM) in methanol-d_4, the complete

https://doi.org/10.1021/jacs.2c02619
J. Am. Chem. Soc. 2022, 144, 8756−8769

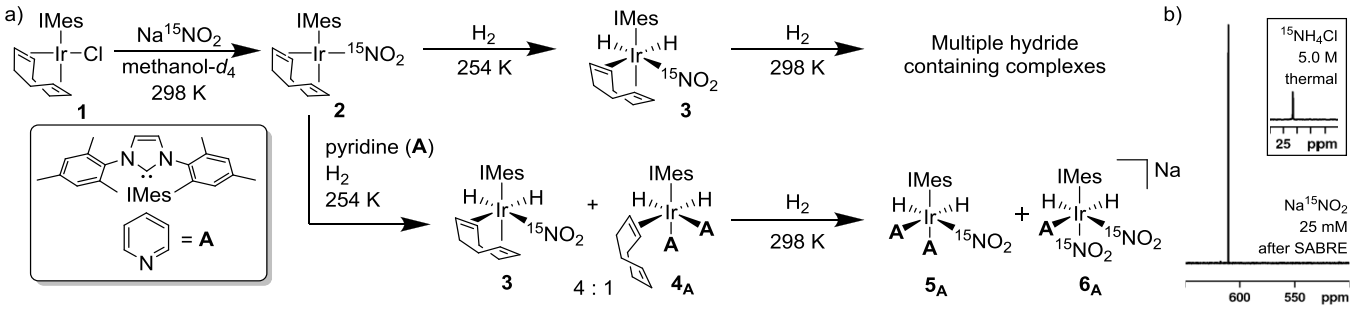

Figure 1. (a) Reaction of [IrCl(COD)(IMes)] with $Na^{15}NO_2$ in the presence of hydrogen and pyridine (inset: structure of the IMes and pyridine ligand). (b) ^{15}N NMR spectrum of $Na^{15}NO_2$ after SABRE hyperpolarization under 3 bar p-H_2 (inset: thermally polarized ^{15}N NMR spectrum of a 5.0 M solution of $^{15}NH_4Cl$ in D_2O for comparison).

conversion to [Ir($^{15}NO_2$)(COD)(IMes)] (**2**) at 298 K (Figure 1a) is observed. This change was readily evident as the ^{15}N signal for free $Na^{15}NO_2$ at δ_N 611.8 moved to δ_N 490.7 for the bound NO_2^- at 255 K (see the Supporting Information). When **2** was then exposed to a 3 bar pressure of H_2 at 254 K, the oxidative addition of hydrogen took place to form [Ir(H)$_2$($^{15}NO_2$)(COD)(IMes)] (**3**). This complex exhibits ^1H NMR for its hydride ligands at δ_H −18.77 (hydride *trans* to $^{15}NO_2^-$, $^2J_{HN}$ = 23.1 Hz and $^2J_{HH}$ = 3.3 Hz) and δ_H −14.17 (hydride *trans* to COD, $^2J_{HH}$ = 3.3 Hz). Additionally, a signal for bound $^{15}NO_2^-$ appears at δ_N 476.1. Hence, there is a strong hydride-^{15}N coupling in this material that would be commensurate with SABRE. Subsequently, this sample was warmed to 298 K for 20 min. This led to the formation of multiple hydride-containing products, some of which display PHIP on exposure to p-H_2 (see the Supporting Information). Pleasingly, a hyperpolarized signal for free $Na^{15}NO_2$ is observed at 298 K in the ^{15}N NMR spectrum after SABRE transfer at −5 mG; a field in the mG range will be needed for efficient SABRE transfer.[51,55,56] The resulting ^{15}N signal enhancement was 134-fold and confirms reversible binding of NO_2^-. Unfortunately, when this sample was left at room temperature for >2 h, SABRE activity was lost because of catalyst decomposition. Hence, we sought to create alternative catalysts that would not only improve the ^{15}N signal enhancement level but also be suitable for repeated measurement over long periods. Coligands have been used to achieve stability in conjunction with weakly binding substrate,[40,41,73] to reduce spin dilution[42,75,76] and to create hydride ligand chemical, rather than magnetic, inequivalence.[77] Hence, we chose to follow this path as it offers a multitude of benefits to SABRE.

Thus, a sample containing [IrCl(COD)(IMes)] (**1**, 5 mM), $Na^{15}NO_2$ (5 equiv), and pyridine (3 equiv) was investigated by NMR spectroscopy. The initial formation of [Ir($^{15}NO_2$)(COD)(IMes)] (**2**) was indicated. Clearly, nitrite outcompetes pyridine for the [Ir(COD)(IMes)]$^+$ center. Subsequently, exposing this sample to 3 bar H_2 at 254 K led again to the formation of neutral **3**. Characterization data are provided in the Supporting Information. We note that known [Ir(H)$_2$(IMes)(η^1-COD)(pyridine)$_2$]Cl (**4$_A$**) forms alongside **3** in a 1:4 ratio. After warming the sample for 1 h at room temperature, further reaction to form two additional hydride-containing products takes place. Of these, [Ir(H)$_2$($^{15}NO_2$)(IMes)(pyridine)$_2$] (**5$_A$**), with characteristic hydride peaks at δ_H −21.24 and −22.45, dominates. The former resonance exhibits a $^2J_{NH}$ splitting of 29 Hz, and both show $^2J_{HH}$ couplings of −8 Hz.

A further minor product formed in this reaction proved to be Na[Ir(H)$_2$($^{15}NO_2$)$_2$(IMes)(pyridine)] (**6$_A$**). It yields hydride resonances at δ_H −22.02 ($^2J_{NH}$ = 29 Hz) and −23.01 with mutual $^2J_{HH}$ splittings of −7 Hz. Interestingly, no evidence for the formation of *tris* pyridine-containing [Ir(H)$_2$(IMes)(pyridine)$_3$]Cl was observed[78] and unlike the complexes formed in the absence of pyridine, pyridine-derived **5$_A$** and **6$_A$** proved stable when left at room temperature for >24 h. Given this stability, these species were suitable probes for rigorous assessment of their SABRE performance. When the ratio of $Na^{15}NO_2$ to pyridine was set to 5:3, the ratio of **5$_A$** to **6$_A$** in solution proved to be 85:15. Further addition of $Na^{15}NO_2$ (25 equiv), while maintaining the pyridine concentration, only moderately shifted the equilibrium between **5$_A$** and **6$_A$** to 80:20 thereby confirming that neutral [Ir(H)$_2$($^{15}NO_2$)(IMes)(pyridine)$_2$] (**5$_A$**) is the most thermodynamically stable of these products.

SABRE Assessment of [Ir(H)$_2$($^{15}NO_2$)(IMes)(A)$_2$] (5$_A$) and Na[Ir(H)$_2$($^{15}NO_2$)$_2$(IMes)(A)] (6$_A$) Activity. In order for effective SABRE, the lifetime of the active catalyst must match with the propagating couplings and a level anticrossing condition should be met.[43,44,46] To assess the SABRE performance of **5$_A$** and **6$_A$**, a series of shake and drop measurements were undertaken using a mu-metal shield to attenuate the Earth's field by a factor of 300 to bring it into the range needed for efficient transfer. These measurements involved first exposing an NMR tube equipped with a *J*. Youngs Tap containing a solution of [IrCl(COD)(IMes)] (**1**, 5 mM), $Na^{15}NO_2$ (5 equiv), and pyridine (4 equiv) in methanol-d_4 (0.6 mL) to H_2 (3 bar) for 1 h to form an 85:15 ratio of **5$_A$** to **6$_A$** in solution. Subsequently, the H_2 atmosphere was replaced with p-H_2 (3 bar), and the sample was shaken for 10 s inside the mu-metal shield. After shaking, the sample was transferred into the 9.4 T detection field and an ^{15}N NMR spectrum was recorded immediately.

Spectral analysis revealed that the free ^{15}N signal of $Na^{15}NO_2$ was now ∼880-fold larger than that of the corresponding thermally polarized NMR spectrum, corresponding to a 0.29% ^{15}N polarization level (Figure 1b). SABRE transfer to the ^{15}N of unlabeled pyridine was also observed, and a 172-fold signal gain was quantified for its resonance at δ_N 301. ^{15}N NMR signals for coordinated NO_2^- ligands were also readily visible at δ_N 511.28 (J_{HN} = 29 Hz) for **5$_A$** and at δ_N 509.7 (J_{HN} = 29 Hz) for the NO_2^- in the equatorial position and at δ_N 483.7 for the ligand in the axial position of **6$_A$**. Repeating the experiment after polarization transfer at 70 G and subsequently recording a ^1H NMR spectrum revealed that PHIP-enhanced hydride resonances for **5$_A$** and **6$_A$**. SABRE hyperpolarization was also quantified for the ^1H resonances of free pyridine as ∼230, 60, and 150-fold for its *ortho*, *meta*, and *para* positions, respectively, after 60 G transfer. No evidence for a PHIP-enhanced hydride resonance for

https://doi.org/10.1021/jacs.2c02619
J. Am. Chem. Soc. 2022, 144, 8756−8769

$[Ir(H)_2(IMes)(py)_3]Cl$ at δ_H −22.7 was observed. We conclude therefore that $^{15}NO_2^-$ sensitization is possible through the action of this coligand-supported catalyst.

Effect of Polarization Transfer Field on the Level of ^{15}N NMR Signal Gain in $Na^{15}NO_2$. To improve the levels of signal gain, a more precise polarization transfer field needs to be used. To investigate this effect, a sample containing [IrCl(COD)(IMes)] (**1**, 5 mM), $Na^{15}NO_2$ (5 equiv), and pyridine (4 equiv) in methanol-d_4 (0.6 mL) was exposed to *p*-H_2 (3 bar), and polarization transfer fields from +10 to −10 mG were deployed; these were created by a solenoid located within an mu-metal shield. A profile of the resulting SABRE enhanced resonance for $Na^{15}NO_2$ is presented in the Supporting Information. The highest signal enhancements were observed when the polarization transfer field was nominally +5 or −3 mG with gains of 1948 and 2054-fold, respectively. More precise probing of the polarization transfer field around these maxima revealed that improvement could be achieved using a −3.5 mG value. At this polarization transfer field, a 2329-fold signal gain was quantified through subsequent measurement at 9.4 T which corresponds to an ^{15}N polarization level of 0.77%.

Effect of the Coligand on SABRE Catalysis. To form $\mathbf{5_A}$ and $\mathbf{6_A}$, $^{15}NO_2^-$ must out-bind the stabilizing coligand pyridine. Consequently, we hypothesized that the SABRE processes will be sensitive to the identity of this coligand; such a behavior has been observed previously during the SABRE polarization of sodium pyruvate by sulfoxides,[39] and there are other examples.[41,72,79] Additionally, isotopic labeling of these coligands, which reduces the number of polarization-acceptor spins at the metal center, has proven beneficial while additionally attenuating the effect of relaxation.[42,80,81] A suitable range of coligands were therefore examined to test if it were possible to improve the measured polarization levels in free $Na^{15}NO_2$, as detailed in Figure 2.

In each case, samples containing [IrCl(COD)(IMes)], $Na^{15}NO_2$ (25 equiv), and the coligand (**A**-**H**, 4 equiv) were prepared and then exposed to 3 bar H_2 at 298 K for 1 h to form the corresponding complexes **6** and **7**. Subsequently, a sample was exposed to 3 bar *p*-H_2, in a −3.5 mG field, prior to its rapid insertion into the 9.4 T detection field. The second coligand tested was ^{15}N labeled pyridine (**A**-^{15}**N**), and this reduced the signal enhancement level for $Na^{15}NO_2$ from 2329-fold to 2107-fold. This is likely to reflect the increase in spin dilution associated by increasing the proportion of spin-1/2 nuclei that can accept polarization. The resonance for free ^{15}N-pyridine at δ_N 301 now exhibits a signal gain of 1558-fold. In contrast, the use of pyridine-d_5 (**A**-$\boldsymbol{d_5}$) improves the SABRE hyperpolarization for $Na^{15}NO_2$ as the new enhancement level increases to 3007-fold. As expected, all the pyridine isotopologues yield analogous complexes, **5** to **6**, in a common 85:15 ratio. Hence, catalyst speciation is constant and the ca. 30% improvement, compared to undeuterated **A**, likely reflects both slower relaxation in the active catalyst and reduced polarization.

To further modulate the coligand, other pyridyl derivatives having different steric and electronic properties were examined. Recently reported 2,6-lutidine (**B**)[82,83] was chosen as its *ortho* methyl groups hinder binding to the metal center, a change which might promote ligand loss. When **B** is employed with $Na^{15}NO_2$, an increase in the SABRE polarization level is indeed observed when compared to pyridine. Interestingly, the ratio of $\mathbf{5_B}$ to $\mathbf{6_B}$ has changed to 95:5. However, slow activation means that **3** (c.f. Figure 1a) is still visible after 1 h at room temperature; at this stage, it exists in a 1:1 ratio with $\mathbf{5_B}$. Unfortunately, when

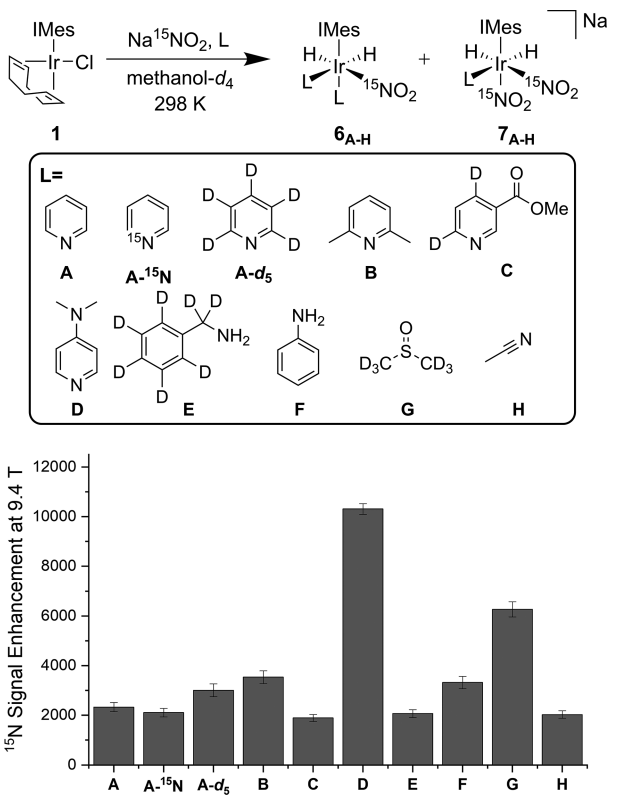

Figure 2. Graphical representation of the effect the coligand, **A**-**H**, has on the resulting SABRE polarization efficiency for $Na^{15}NO_2$ based on the precatalyst [IrCl(COD)(IMes)], $Na^{15}NO_2$ (25 equiv), and coligand (4 equiv) in methanol-d_4 at 298 K. The ^{15}N NMR signal enhancements occur after polarization transfer from 3 bar *p*-H_2 in a −3.5 mG field.

this sample is left under a 3 bar atmosphere of H_2 for a longer time to allow full activation, sample degradation and the formation of multiple hydride-containing complexes are noted. Hence, **B** fails to provide the stability needed.

The use of electron-deficient methyl 4,6-d_2-nicotinate (**C**), which has been shown to exhibit ^1H polarization levels of ca. 60% itself under SABRE,[42,60] as a coligand was found to decrease the signal enhancement of $Na^{15}NO_2$ to 1894. The formation of mono-**C**-substituted $\mathbf{6_C}$ is favored by this change as the ratio of $\mathbf{5_C}$ to $\mathbf{6_C}$ became 1:2. In contrast, electron-rich dimethylamino pyridine (**D**, DMAP) forms $\mathbf{5_D}$ in a 17:1 ratio with $\mathbf{6_D}$. Consequently, electron-donating coligands favor the formation of a *bis*-co-ligand substituted complex. Additionally, a significantly improved 10,313-fold ^{15}N signal enhancement is now observed for $Na^{15}NO_2$ which corresponds to the creation of a 3.4% ^{15}N polarization level.

Nonheterocyclic ligands can also be utilized for SABRE. As such, amine ligands have been shown to be able to form stable SABRE catalysts and are effective agents for SABRE-relay polarization transfer.[80,81,84−86] When utilized as a coligand for the hyperpolarization of $Na^{15}NO_2$, benzylamine-d_7 (**E**-$\boldsymbol{d_7}$) led to a ^{15}N signal gain of 2070-fold. The two hydride-containing complexes $\mathbf{5_E}$ and $\mathbf{6_E}$ were formed under these conditions in a ca. 1:1 ratio with hydride resonances at δ_H −22.10 and −23.40 and δ_H −22.36 and −22.72, respectively. When aniline (**F**) was used as the coligand, a 3322-fold signal gain for $Na^{15}NO_2$ was quantified. In this sample, $\mathbf{5_F}$ now dominates.

Similarly, sulfoxides have proven to be efficacious for the hyperpolarization of sodium pyruvate and weakly coordinating

https://doi.org/10.1021/jacs.2c02619
J. Am. Chem. Soc. 2022, 144, 8756−8769

substrates.[39,40,79,87] The coligand DMSO-d_6 (**G**) gave a 6270-fold signal enhancement for $Na^{15}NO_2$. Interestingly, while $Na[Ir(H)_2(^{15}NO_2)_2(IMes)(DMSO\text{-}d_6)]$ ($\mathbf{6_G}$) is now dominant, a second isomer $\mathbf{7_G}$, where the two $^{15}NO_2$ ligands lie *cis* to one another and *trans* to hydride is observed. This complex gives rise to a single hydride resonance at δ_H −22.32 where $J_{NHcis} + J_{NHtrans}$ is 27.6 Hz. The $^{15}NO_2$ resonance of $\mathbf{7_G}$ appears at δ_H 502. Isomer $\mathbf{5_G}$ is also detected, but now as a minor species, with the ratio of $\mathbf{5_G}$:$\mathbf{6_G}$:$\mathbf{7_G}$ in solution being ∼1:9:5. Characterization data for these complexes are provided in the Supporting Information. Finally, acetonitrile[88] gave a 2029-fold ^{15}N signal gain for NO_2^-. For acetonitrile, the neutral complex $[Ir(H)_2(^{15}NO_2)(IMes)(acetonitrile)_2]$ ($\mathbf{5_H}$), with hydride resonances at δ_H −22.66 ($^2J_{NH}$ = 26.7 Hz, $^2J_{HH}$ = −7 Hz) and −21.77 ($^2J_{HH}$ = −7 Hz), was the only complex observed. Clearly substantial coligand effects occur, with **D** proving optimal.

Identifying the Optimum DMAP (D):$Na^{15}NO_2$ Ratio. Interestingly, this ligand yielded the highest concentration of isomer **5**. We postulated that the concentration of $\mathbf{5_D}$ in solution could be further manipulated by changing the number of equivalents of **D** in relation to [IrCl(COD)(IMes)] (**1**) and $Na^{15}NO_2$. Therefore, a series of samples were prepared with between 3 and 20 equiv of **D** relative to **1**. After activation, they were exposed to 3 bar p-H_2 while located in a −3.5 mG polarization transfer field. The resulting signal enhancements at 9.4 T are shown in the Supporting Information.

When three equivalents of **D** (with respect to iridium) are utilized, a 9086-fold signal enhancement is observed with the corresponding $\mathbf{5_D}$:$\mathbf{6_D}$ ratio being 8:1. Increasing the concentration of DMAP to four equivalents improved the signal gain seen at 9.4 T to 11,019-fold. The ratio of complex $\mathbf{5_D}$:$\mathbf{6_D}$ also increased to 17:1. Further incremental increases in DMAP concentration, to 6, 8, and 10 equiv, gave signal enhancements of 12,036, 12,079, and 11,888-fold, respectively. The ratio $\mathbf{5_D}$:$\mathbf{6_D}$ was now 24:1 in all three samples. At higher loadings of **D**, the formation of $[Ir(H)_2(IMes)(\mathbf{D})_3]Cl$ is observed, as a single hydride resonance at δ_H −23.00. Clearly, this catalyst does not transfer hyperpolarization to $Na^{15}NO_2$ and hinders the overall ^{15}N signal gain because of consumption of p-H_2. Therefore, we conclude that a sensible DMAP level lies between 6 and 10 equivalents with respect to iridium. This creates SABRE beneficial $\mathbf{5_D}$ as the dominant species in solution.

Synthesis and Utilization of DMAP-d_2 for SABRE. As stated, deuteration of ligands within the active catalyst can be beneficial.[42,70,76,77,88] We postulated that deuteration of the *ortho* protons in **D**, to give DMAP-d_2, may lead to further improvements in ^{15}N polarization. Thus, DMAP-d_2 was synthesized via H/D exchange from DMAP in D_2O under microwave irradiation as reported in the literature.[89] Examination of a sample containing [IrCl(COD)(IMes)] (5 mM), DMAP-d_2 (6 equiv), and $Na^{15}NO_2$ (25 equiv) in methanol-d_4 and exposure to 3 bar p-H_2 at a polarization transfer at −3.5 mG led to a signal gain of 13,811 after investigation at 9.4 T (4.56% ^{15}N polarization level). The corresponding value with ^1H-DMAP was 12,036, and hence introducing the ^2H is beneficial to SABRE.

Effect of NHC Identity on the Efficiency of $Na^{15}NO_2$ Polarization. Aiming to improve the polarization outcome still further, a study of the effect of the NHC ligand was completed in conjunction with DMAP-d_2. Previously, we have shown how manipulation of the steric and electronic properties of this ancillary ligand can result in improved ^1H, ^{13}C, and ^{15}N signal enhancements because of changes in the rate of ligand exchange.[60] We sequentially increased the steric bulk of the NHC (quantified by the magnitude of %BurV[90,91]) to drive ligand exchange (Figure 3). On moving from the IMes ligand (%BurV = 31.2) to SIMes (32.7), we saw a 14,628-fold signal gain which is a slight improvement from the 13,811-fold signal gain previously observed for IMes. IPr (33.6) and SIPr (35.7) both also led to increased signal enhancements of 15,799 and 17,149-fold. However, the best result was obtained for IPent as a 20,337-fold signal gain which has the highest %BurV of 43.4.

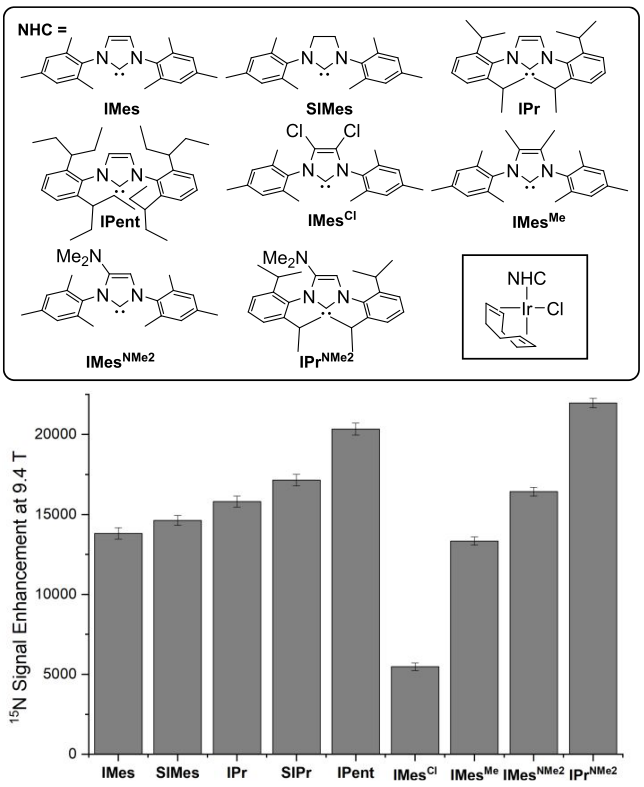

Figure 3. Effect of NHC on the ^{15}N NMR signal gain for $Na^{15}NO_2$ with precatalyst [IrCl(COD)(NHC)] (5 mM), DMAP-d_2 (6 equiv), and $Na^{15}NO_2$ (25 equiv) in methanol-d_4 after polarization transfer at −3.5 mG under 3 bar p-H_2.

Next our focus turned to the electronic properties of the NHC ligand (Figure 3). As expected, electron-deficient $IMes^{Cl}$, which has chloro substituents on the imidazole ring, reduced the signal enhancement to just 5471. Introducing methyl groups on the imidazole ring showed a minimal effect when compared to IMes (13,336-fold vs 13,811-fold, respectively). However, introduction of a single $-NMe_2$ group increased the signal enhancement level to 16,427-fold at 9.4 T.

To combine the steric and electronic effects, we utilized the ligand IPr^{NMe2}, which has previously proven to be effective for Buchwald−Hartwig amination catalysis,[92,93] to form the precatalyst $[IrCl(COD)(IPr^{NMe2})]$. This catalyst system gave the highest ^{15}N signal enhancement for free $Na^{15}NO_2$ seen, 21,967-fold at 9.4 T which is equivalent to 7.2% polarization.

Effect of $Na^{15}NO_2$ Concentration on Signal Enhancement. A series of samples were prepared which contained varying excesses of $Na^{15}NO_2$ relative to 5 mM of $[IrCl(COD)(IPr^{NMe2})]$ and a constant 30 mM of DMAP-d_2. The corresponding hyperpolarization results are presented in the Supporting Information. Reducing the substrate excess to 10 equiv with respect to iridium increased the ^{15}N signal enhancement to 36,629-fold, but for just 4 equiv a value of

https://doi.org/10.1021/jacs.2c02619
J. Am. Chem. Soc. 2022, 144, 8756−8769

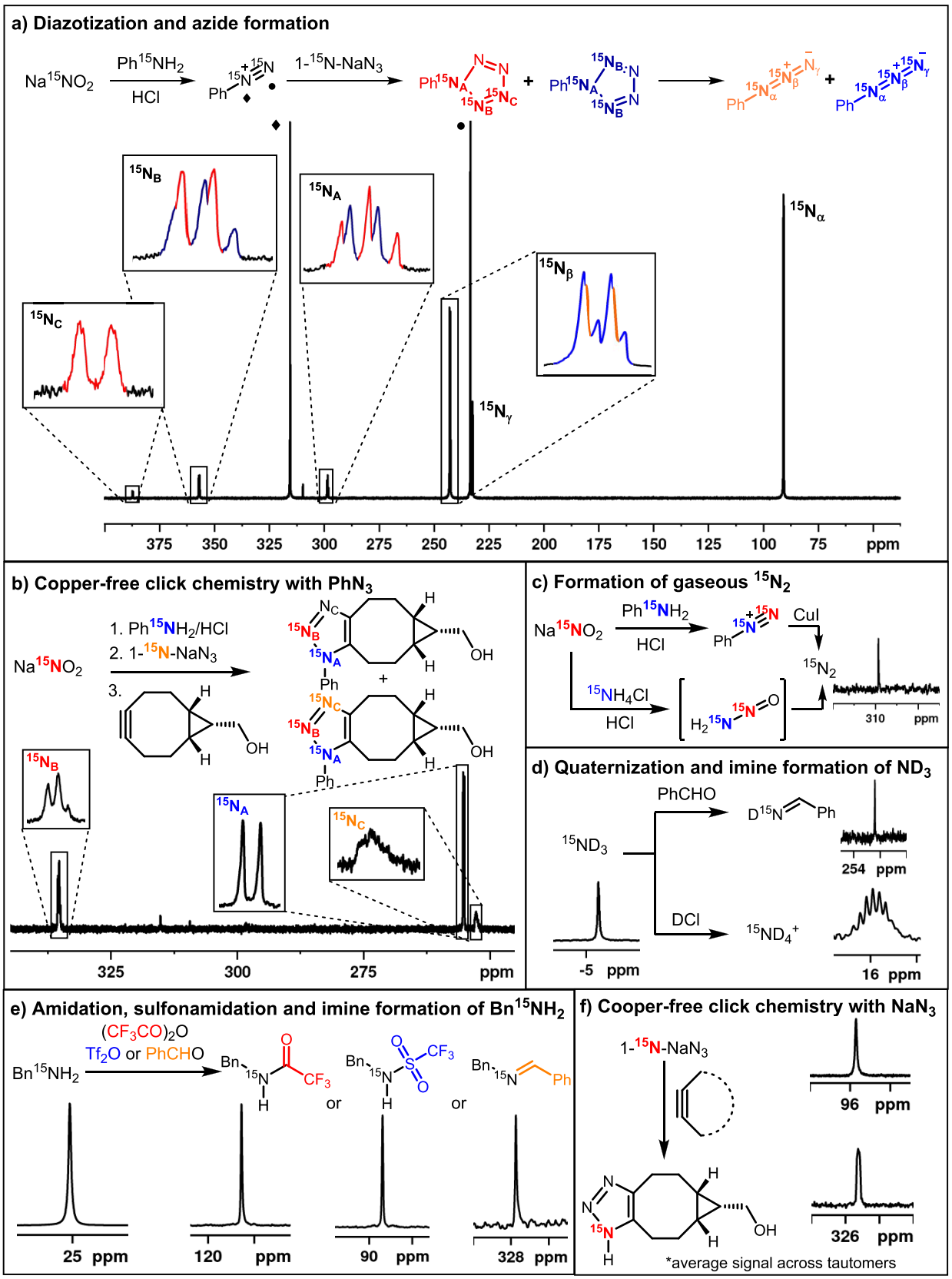

Figure 4. Establishing SABRE hyperpolarization allows the reactivity of ^{15}N-containing synthons to be assessed. (a) Multistep reaction from $Na^{15}NO_2$ that tracks diazotization with aniline-^{15}N and the subsequent formation of two isotopomers of phenyl azide after reaction with 1-^{15}N-NaN_3 in a process that proceeds through a cyclic intermediate; (b) copper-free click reaction of PhN_3 formed as in part (a); (c) formation of N_2(g); (d) ND_3 quaternization with DCl(aq) and imine formation with benzaldehyde; (e) amidation, sulfonamidation, and imine formation of benzylamine-^{15}N; (f) copper-free click reaction of 1-^{15}N-NaN_3.

https://doi.org/10.1021/jacs.2c02619
J. Am. Chem. Soc. 2022, 144, 8756−8769

62,470-fold was found which is equivalent to 20.6% ^{15}N polarization. Conversely, increasing the substrate loading to 50 equiv reduced the signal gain to 10,382 (3.17%), albeit with an improved signal to noise ratio. When the concentration of [IrCl(COD)(IPr^{NMe2})] is reduced to 0.25 mM, while maintaining the 1:4 molar ratio with Na$^{15}NO_2$, the ^{15}N polarization level increases to 28.42%. This phenomenon is likely the result of increasing the excess of *p*-H_2, the limiting reagent, relative to this substrate.[53,60]

Detection of Unlabeled $NaNO_2$. Given the high signal gains obtained for Na$^{15}NO_2$, we tested a sample where the ^{15}N label was present at natural abundance. This sample contained 20 mM of $NaNO_2$ and was examined with [IrCl(COD)(IPr^{NMe2})] (5 mM) and DMAP-d_2 (6 equiv,). An ^{15}N signal was easily seen whose signal enhancement was 115,592-fold at 9.4 T; this corresponds to a 38.1% polarization level.

Effect of 15-Crown-5 and Alternative Solvents. Unfortunately, the ionic nature of $NaNO_2$ acts to limit its solubility in the range of organic solvents that are typically employed for SABRE catalysis; it has a moderate solubility in methanol; however, it is sparingly soluble in other primary alcohols and insoluble in most apolar solvents. In an attempt to increase methanol-d_4 solubility, the macrocycle 15-crown-5 was added, which has a high chelating affinity for Na^+.[94,95] SABRE transfer was therefore undertaken on a sample containing [IrCl(COD)(IMes)] (5 mM), Na$^{15}NO_2$ (25 equiv), DMAP (6 equiv), and 15-crown-5 (25 equiv) in methanol-d_4. This led to an ^{15}N signal enhancement of 12,044-fold at 9.4 T for $^{15}NO_2^-$ which corresponds to 3.97% and reflects a 10% improvement over the analogous measurement with no 15-crown-5. Interestingly, the ratio of $\mathbf{5_D}$ to $\mathbf{6_D}$ in solution was 99:1, as opposed to 91:9 seen in the absence of 15-crown-5. For the optimized catalyst and coligand ([IrCl(COD)(IPr^{NMe2})] (5 mM), Na$^{15}NO_2$ (25 equiv), and DMAP-d_2 (6 equiv)), the effect of 15-crown-5 proved to be less pronounced, with the ^{15}N signal gain improving from 21,967-fold to just 23,114-fold. Hence, solvent effects on this catalysis are substantial and likely to change ligand exchange rates in addition to catalyst speciation.

When an NMR sample containing [IrCl(COD)(IMes)] (5 mM), Na$^{15}NO_2$ (25 equiv), and **D** (6 equiv) was prepared in dichloromethane-d_2 (0.6 mL), the impact of insolubility of Na$^{15}NO_2$ was immediately evident. After sonication for 30 min, the sample was exposed to H_2 (3 bar). Investigation by NMR spectroscopy revealed just [Ir(H)$_2$Cl(IMes)(DMAP)$_2$]. However, when an analogous sample was prepared containing 15-crown-5 in a 1:1 ratio with Na$^{15}NO_2$, a different hydride-containing complex formed. Its hydride resonances appear at δ_H −22.66 ($^2J_{HN}$ = 27.5 Hz and $^2J_{HH}$ = −7 Hz) and δ −23.00 ($^2J_{HH}$ = −7 Hz) and match those of $\mathbf{5_D}$. After SABRE transfer in a −3.5 mG field, a 3586-fold signal enhancement was observed at 9.4 T for the free $^{15}NO_2^-$ resonance at δ_N 618. Warming this sample to 308 K prior to polarization transfer significantly improved the signal gain to 7248-fold and indicates that slow ligand exchange limits the polarization level attained. However, warming further to 323 K yielded no further increase. Using the electron-rich and sterically encumbered precatalyst [IrCl(COD)(IPr^{NMe2})] also yielded improved polarization transfer as an 8149-fold signal gain is seen at 9.4 T. Warming this sample, however, had no benefit. Hence, we have demonstrated how significant polarization levels for $^{15}NO_2^-$ result in dichloromethane-d_2 if 15-crown-5 is present.

Assessment of Na$^{15}NO_2$ Relaxation Rates. DNP hyperpolarized Na$^{15}NO_2$ is reported to have a T_1 of 14.8 s in D_2O at 5.8 T.[15] We used a low-tip angle approach to assess the T_1 of this SABRE-polarized product at 9.4 T. It was found to be comparable at 16.45 s in the presence of a SABRE catalyst. This value was also determined using an automated hyperpolarization device under reversible flow,[96] after first conducting the SABRE process at −3.5 mG, prior to turning off the *p*-H_2 supply and holding the sample in a defined magnetic field for a period of time, prior to transfer to 9.4 T to acquire a spectrum. Repeating this process for a number of time points enables the effective low field T_1 value to be calculated. This analysis was undertaken on samples that were stored in the mu-metal shield (ca. 300-fold shielding) or at −3.5 mT. The new T_1 values were 14.9 and 11.2 s, respectively (see the Supporting Information). These values suggest that there will be sufficient time to use the hyperpolarized $^{15}NO_2^-$ resulting from SABRE synthetically to create other hyperpolarized products as $3 \times T_1$ is available before a signal vanishes. Interestingly, as the T_1 values for ^{15}N nuclei can dramatically be extended when they are located in an appropriate magnetic field, accessing reaction times of many minutes may be possible.[55,97,98] We are currently exploring this, but here we show how rapid reactions can be evaluated through ^{15}N NMR at high field is detailed in the following sections.

Conversion of Hyperpolarized Na$^{15}NO_2$ to a Diazonium via NO^+. The first reaction we consider is the important Sandmeyer reaction that rapidly converts arylamines into arylhalides via a diazonium salt intermediate.[99] Since the first reported example in 1884,[100] it has become a mainstay of organic chemistry and many related reactions have been discovered.[101] Classically, it utilizes either stoichiometric or catalytic amounts of a copper halide, although a number of metal free variants are known.[102−104] The formation of the diazonium salt intermediate proceeds via nitrous acid addition, which is formed in situ from the reaction of $NaNO_2$ and a strong acid. We sought to follow a diazotization reaction by ^{15}N hyperpolarized NMR spectroscopy. To do this, we first created a solution of hyperpolarized Na$^{15}NO_2$ using the previously optimized conditions ([IrCl(COD)(IPr^{NMe2})] (5 mM), DMAP (30 mM), Na$^{15}NO_2$ (125 mM) in methanol-d_4 (0.6 mL)). A solution of aniline (150 mM) and conc. HCl (100 μL) in methanol-d_4 (100 μL) was then added, and the resulting NMR tube was immediately transferred into the spectrometer and investigated using a T_1-corrected variable flip angle pulse sequence. It took between 3 and 5 s to start this series of measurements, and the resulting hyperpolarized signals were indicative of nitrous acid (H$^{15}NO_2$, δ_N 563) forming phenyl diazonium chloride (δ_N 314) and *ortho*-$^{15}N_2$ (δ_N 308). Their identity was confirmed by their independent synthesis and comparison to literature data.[105] Over the course of 30 s, the response for H$^{15}NO_2$ vanished.

When this process was repeated with aniline-^{15}N, the reaction monitoring step revealed the detection of hyperpolarized responses for both of the ^{15}N centers in the diazo product at δ_N 315.0 and 232.6 in agreement with the literature (Figure 4a).[106] The hyperpolarization of both of the ^{15}N sites happens even though aniline itself was not hyperpolarized. Consequently, efficient polarization transfer between them takes place during their time as a coupled spin pair at low field. As a control, we exposed a sample of phenyl diazonium chloride and the catalyst to *p*-H_2 at −3.5 mG and noted no hyperpolarized ^{15}N resonance result. Consequently, all the hyperpolarized signals seen during

https://doi.org/10.1021/jacs.2c02619
J. Am. Chem. Soc. 2022, 144, 8756−8769

this reaction originate from the initially hyperpolarized $Na^{15}NO_2$ synthon.

Figure S12 of the Supporting Information details how the hyperpolarization level of unlabeled $NaNO_2$ is sufficient to allow the detection of phenyl diazonium chloride without the need for isotopic labeling.

Reactions of Hyperpolarized $^{15}N_2$-Phenyl Diazonium Chloride. Phenyl diazonium chloride proved to have hyperpolarized T_1 values for $^{15}N_1$ and $^{15}N_2$ of 29.4 and 39.2 s, respectively, at 9.4 T. Additionally, it proved to be relatively stable under these conditions as only limited decomposition to hyperpolarized $^{15}N_{2(g)}$ (δ_N 308) was seen. This meant that we could explore the reactivity of this diazonium salt in situ. It is known that such salts liberate N_2 under photochemical or transition-metal-catalyzed processes.[107,108] Under our hyperpolarized regime, addition of CuI saw its rapid conversion into N_2 and consequently a strong signal was seen at δ_N 308.

A similar hyperpolarized diazonium salt solution was prepared and then treated with NaN_3 to examine the formation of phenyl azide. Rapid monitoring enabled the collection of a hyperpolarized ^{15}N NMR spectrum with strong resonances at δ_N 242.2 and 90.1 that share a common $^2J_{NN}$ of 13.8 Hz because of this species. According to the literature, this reaction could proceed via a cyclic and/or acyclic intermediate, species which would deliver five and three distinct ^{15}N signals, respectively.[109−111] Interestingly, we detect transient signals at δ_N 356.8 and 298.2 (both with $^2J_{NN}$ = 16.7 Hz) for the site connected to the C_6H_5 ring which we assign to this product. Upon repeating this study with 1-^{15}N NaN_3, these two signals gain further complexity and appear alongside one other at δ_N 387.3 (d, 17 Hz). These additional features are reflective of the two possible isotopologues that can result from $^{15}N_1-N_3^-$ addition to form a cyclic intermediate, which place a Ph−^{15}N next to two chemically equivalent ^{15}N groups (a triplet at δ_N 298.6 of 17 Hz is seen for it alongside a doublet of 17 Hz at δ_N 356.9) or one (a doublet at δ_N 298.6 of 17 Hz is now seen) alongside a further triplet at 356.9 of 17 Hz and a doublet at δ_N 387.3 (d 17 Hz) for the next and more remote center (Figure 4a) ^{15}N of the N_5 ring. Hence, all three unique signals for this cyclic intermediate have been detected. We note that its conversion into phenyl azide (Ph$-^{15}N=^{15}N^+=^{15}N^-$ and Ph$-^{15}N=^{15}N^+=N^-$) proceeds rapidly at 298 K, and the signals for this product also appear, δ_N 90.3, 242.5, and 232, with apparent T_1 values of 56, 192, and 101 s at 9.4 T, all respectively.

These long T_1 values enable the creation of strongly hyperpolarized phenyl azide. When the reactive alkyne, (1*R*,8*S*,9*s*)-bicyclo[6.1.0]non-4-yn-9-ylmethanol,[112] is added to this hyperpolarized sample in a third synthetic step, further reaction to form the corresponding triazole occurs. Despite the corresponding ^{15}N signal's T_1 in this product proving to be <10 s, its formation is readily indicated in the associated hyperpolarized ^{15}N NMR measurements through three signals at δ_N 335.4, 255.3, and 252.7 that can be linked through mutual $^2J_{NN}$ couplings of 12.8 Hz (Figure 4b). As copper-free click chemistry is used widely for bioconjugation with nuclei acids, we expect such measurements to help in the optimization of pharmaceutical preparations and/or in vivo detection.[113,114]

These data have clearly illustrated the successful examination of a multistep reaction as it proved possible to simultaneously see ^{15}N signals for the phenyl diazonium salt, the pentazole intermediate and phenyl azide (Figure 4a) or the pentazole intermediate, phenyl azide, and the triazole (Figure 4b). We plan to develop methods to extract precise kinetic data for these changes in the future.

Conversion of Hyperpolarized $Na^{15}NO_2$ to $^{15}N_2$ through Reaction with $^{15}NH_4Cl$/HCl. N_2 gas spontaneously forms from the diazonium salts of primary amines. Consequently, as $^{15}NH_4Cl$ is readily available we monitored its reaction with $Na^{15}NO_2$ and saw strong signals for $^{15}N_2$ in solution (see Figure 4c). We have therefore detailed two facile approaches to hyperpolarized $^{15}N_2$, we are currently exploring as routes to potentially important *p*-N_2.[54,74]

Utilization of ^{15}N Hyperpolarized Azide, Amines, and Ammonia as Probes of Reactivity. The SABRE hyperpolarization of NH_3 and amines, such as benzylamine, and their use in SABRE-relay have been extensively reported.[80,81,84−86] Additionally, ammonia and amines have been used as a coligand that leads to improved SABRE catalysis.[62,115] The ^{15}N polarization of benzylamine-^{15}N (**E**-^{15}**N**) is reported to be ca. 800-fold at 9.4 T.[84] This involves the action of $[Ir(H)_2(IMes)(\mathbf{E}\text{-}^{15}\mathbf{N})_3]Cl$ in dichloromethane-d_2 solution. We restudied this process to improve the SABRE outcome and thereby provide access to a further functional group to demonstrate hyperpolarized reactivity screening. Using the same conditions as previously reported ([IrCl(COD)(IMes)] (5 mM) and benzylamine-^{15}N (**E**-^{15}**N**, 7 equiv)), we determined that optimal SABRE transfer occurs at −4 mG. At this transfer field, a 7751-fold signal enhancement was achieved at 9.4 T. As the rate of benzylamine dissociation from $[Ir(H)_2(IMes)(\mathbf{E}\text{-}^{15}\mathbf{N})_3]Cl$ in dichloromethane-d_2 is slow,[45,85] we found that warming the sample to 308 K further improved the enhancement level to 11,211-fold which corresponds to 3.7% ^{15}N polarization; it has 14 s T_1 at 9.4 T in the absence of the catalyst and 12.8 s when it is present. We predict that further optimizations could improve this value; however, the resulting signal strengths are sufficient to explore its reactivity. We exemplify now the utilization of hyperpolarized **E**-^{15}**N** as a synthon for amidation, sulfonamidation, and imine formation. This resulted in the ^{15}N detection of the products shown in Figure 4e. Their identity was verified by independent synthesis as described in the Supporting Information or by comparison to literature data. In particular, the addition of trifluoroacetic anhydride to hyperpolarized **E**-^{15}**N** led to the formation and detection of *N*-benzyl-trifluoroacetamide-^{15}N in the resulting ^{15}N NMR spectrum through a signal at δ_N 116.4. Similarly, triflic anhydride reacted to yield the analogous sulfonamide with a resonance at δ_N 88.6. Finally, addition of benzaldehyde to **E**-^{15}**N** produced the imine condensation product as evident from a peak at δ_N 327.7.

Ammonia is also widely used in synthetic chemistry and we sought to test whether its reactivity could be probed while hyperpolarized. As gaseous $^{15}NH_3$ was expensive and difficult to handle, we used an alternative ammonia source.

This involved taking a 1:1 mixture of $^{15}NH_4Cl/KO^tBu$ and adding it to **1** in the presence of H_2 with the result that $[Ir(H)_2(IMes)(^{15}ND_3)_3]Cl$ forms in methanol-d_4. After polarization transfer at −4 mG, a 3268-fold ^{15}N signal gain was quantified for the free $^{15}ND_3$ signal. However, over the course of ca. 1 h, the signal enhancement diminishes when the SABRE process is repeated. In contrast, the use of $^{15}NH_4OH$ (available as a 14 molar solution in H_2O) yielded the same active catalyst, but the sample was now stable for >24 h. The ^{15}N signal enhancement is also slightly improved to 3765-fold. Changing the NHC ligand proved to have a modest effect on SABRE efficacy (see the Supporting Information), and warming the sample derived from **1** to 308 K improved the signal gain to

https://doi.org/10.1021/jacs.2c02619
J. Am. Chem. Soc. 2022, 144, 8756−8769

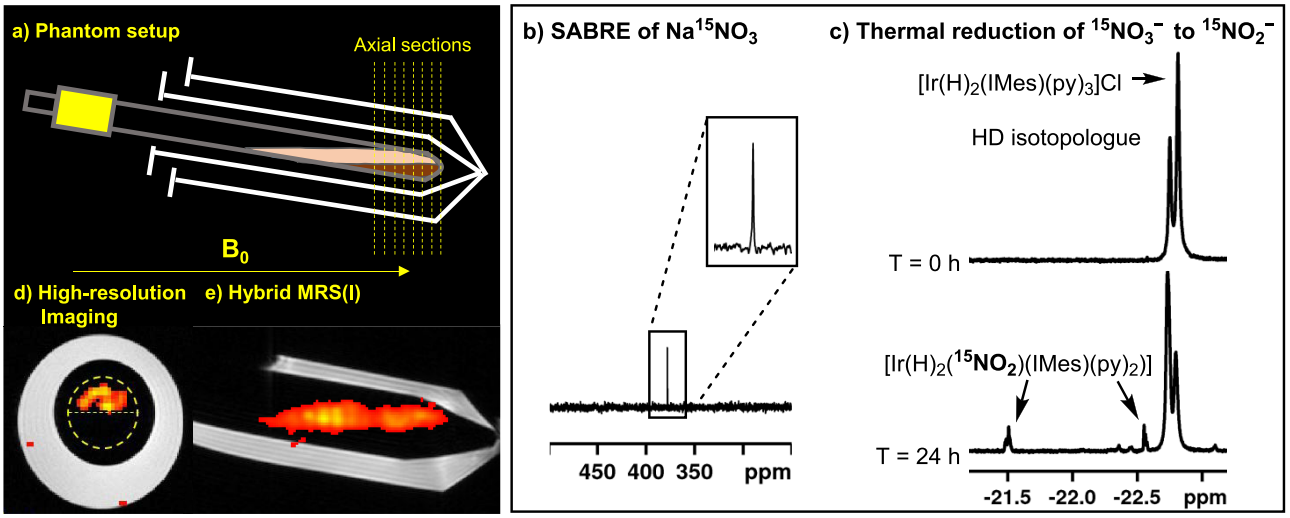

Figure 5. Establishing the imaging capability of SABRE hyperpolarized ^{15}N O_2^- in biocompatible solvents. (a) Setup for hyperpolarized imaging at 7 T of a reaction cell used for the biphasic preparation of $^{15}NO_2^-$; (b) SABRE hyperpolarized ^{15}N NMR spectrum of $Na^{15}NO_3$ created with [Ir(COD)(IMes)(pyridine)]BF_4, DMSO-d_6 (2 equiv), $Na^{15}NO_3$ (25 equiv), and 3 bar p-H_2 at 9.4 T; (c) ^1H NMR spectra of the hydride region establish the conversion of NO_3^- to NO_2^- via the detection of Ir(H)($^{15}NO_2$)(IMes)(py)$_2$]; (d) high-resolution three-dimensional axial acquisition using spiral (out) encoding of 6 cm^3 over a 64 × 64 × 8 matrix with a 6 s acquisition time; (e) hybrid MRS(I) data collected using an EPSI pulse sequence and a 64 × 64 matrix (512 spectral points).

4521-fold. However, dramatic improvements are observed with a coligand. While the coligands DMSO-d_6, CD_3CN, NO_2^-, and DMAP (see the Supporting Information) were explored, pyridine-d_5 proved to give the highest signal gain of 15,145-fold (5.0% polarization). The ^{15}N T_1 value for $^{15}ND_3$ at 9.4 T proved to be 37 s so there is again a wide time window over which a reaction can be examined. Protonation of $^{15}ND_3$ with DCl in D_2O led to the detection of hyperpolarized $^{15}ND_4^+$ as a signal δ_N 15.93 with resolved ^{15}N-D scalar couplings, J_{ND}, of 10.8 Hz and a hyperpolarized T_1 of 33.6 s (Figure 4d).

The SABRE hyperpolarization of 1-^{15}N NaN_3 itself using the coligand strategy with DMAP and **1** also proved successful. The reaction was found to proceed to form [Ir(H)$_2$(DMAP)$_2$(IMes)(^{15}N═N═N)] which exhibits hydride signals at δ_H −23.1 ($^2J_{HH}$ = 8 Hz) and δ_H −25.0 ($^2J_{HH}$ = 8 Hz and $^2J_{NH}$ = 8 Hz) alongside [Ir(H)$_2$(DMAP)$_3$(IMes)]Cl (δ_H −22.8). SABRE transfer at −3.5 mG yielded 3.2% hyperpolarization of the N_3^- signal at δ_N 95.7. A hyperpolarized solution of NaN_3 was then reacted directly with (1*R*,8*S*,9*s*)-bicyclo[6.1.0]non-4-yn-9-ylmethanol to form the triazole. Under these conditions, a single hyperpolarized ^{15}N response for the product was visible at δ_N 321.3 as expected and is shown in Figure 4f.

Producing Hyperpolarized NO_2^- in Water. For biological applications, it is desirable to produce hyperpolarized NO_2^- in water. Unfortunately, $\mathbf{5_A}$ did not form when the analogous reaction was conducted in this solvent. Preforming $\mathbf{5_D}$ in methanol-d_4 prior to removing the solvent and replacing it with D_2O was also unsuccessful. One further way to achieve an aqueous bolus is to use a biphasic[116] approach with dichloromethane-d_2, which could benefit from the fact that the catalyst is not present in the aqueous layer.[65,117] A sample containing [IrCl(COD)(IMes)] (5 mM), $Na^{15}NO_2$ (25 equiv) and DMAP (6 equiv) and 15-crown-5 (25 equiv) in dichloromethane-d_2 (0.3 mL) was prepared and exposed to H_2 (3 bar) to form the active catalyst. D_2O (0.3 mL) was then added under a nitrogen atmosphere. After SABRE transfer at −3.5 mG and phase separation, two hyperpolarized signals were seen in the corresponding ^{15}N NMR spectrum for $Na^{15}NO_2$ at δ_N 618 and δ_N 609. These peaks had relative intensities of 1:70 and were assigned to $Na^{15}NO_2$ dissolved in the dichloromethane-d_2 and D_2O phases respectively by comparison with data from independent solutions. Assuming that all of the $Na^{15}NO_2$ was present, the D_2O layer results in a ^{15}N signal gain of 4667-fold. This will be an underestimate of the actual signal gain. As 15-crown-5 can also play a role as a phase-transfer catalyst,[118] a further 25 equiv was added to the sample and this proved to increase the signal enhancement level to 13,794-fold. Further additions of 15-crown-5 did not improve on this; however, warming the sample to 308 K resulted in a 26,327-fold signal gain at 9.4 T. This is equivalent to an 8.69% polarization level in aqueous $Na^{15}NO_2$. Hence, we have created a simple route to hyperpolarized $Na^{15}NO_2$ in biocompatible water. The level of signal gain compares favorably with the <1% reported with DNP.[15] To confirm the phase distribution of $Na^{15}NO_2$, a series of ^{15}N MRI images were recorded on a 10 mm-diameter sample tube as detailed in the Supporting Information. The data in Figure 5 details these results which confirm both separation and the fact that the associated signal strengths are sufficient to allow for high-sensitivity ^{15}N imaging of NO_2^-.

SABRE Hyperpolarization of $Na^{15}NO_3$. In contrast to nitrite, nitrate is usually noncoordinating; however, there are examples of it functioning as a weak monodentate or bidentate ligand.[29,119−123] To further explore SABRE's use as a tool to polarize materials featuring in the nitrogen cycle, we explored the SABRE hyperpolarization of $Na^{15}NO_3$. As expected, in the absence of a coligand no active SABRE catalyst formed in the reaction between [IrCl(COD)(IMes)] and $Na^{15}NO_3$ under a H_2 atmosphere (3 bar) in methanol-d_4. We screened a number of coligands (DMAP, 2-picoline, DMSO-d_6, DPSO, or CD_3CN) and saw no evidence for the ^{15}N polarization of $Na^{15}NO_3$. In each case, the dominant hydride-containing species in solution was [Ir(H)$_2$(IMes)(coligand)$_3$]Cl or [IrCl(H)$_2$(IMes)-(coligand)$_2$]. However, when the ionic precatalyst [Ir(COD)-(IMes)(pyridine)]BF_4 was used with DMSO-d_6 (2 equiv), a 547-fold signal enhancement for the $^{15}NO_3^-$ signal at 9.4 T

https://doi.org/10.1021/jacs.2c02619
J. Am. Chem. Soc. 2022, 144, 8756−8769

(0.18% ^{15}N polarization) is observed (Figure 5b). No direct evidence for an NO_3^- containing complex could be found, and therefore, polarization transfer must occur through a very low concentration species.

Unexpected Reduction of Sodium Nitrate. During the course of these investigations, a hyperpolarized ^{15}N NMR signal at δ_N 511.28 (J_{HN} = 28.5 Hz) appears over the course of 0.5 h when pyridine alone is used as a coligand. This matches the equatorial NO_2^- resonance previously observed for [Ir(H)$_2$(^{15}NO$_2$)(IMes)(pyridine)$_2$] ($\mathbf{5_A}$). Relatively strong polarized signals for free pyridine and the pyridine ligand *trans* to hydride in [Ir(H)$_2$(IMes)(py)$_3$]Cl (δ_N 299.6 and 255.7, respectively) were also observed in these NMR spectra. As expected, the corresponding ^{1}H NMR spectrum is dominated by the hydride signal of [Ir(H)$_2$(IMes)(py)$_3$]Cl which appears at δ_H −22.7, although a weakly PHIP-enhanced signal for $\mathbf{5_A}$ is visible in this spectrum at δ_H −21.49 (the peak at δ_H −22.71 cannot be observed because of overlap). No evidence for $\mathbf{6_A}$ was observed in either the ^{1}H or ^{15}N NMR spectra which indicates that $\mathbf{5_A}$ is likely to be the kinetic product of this reaction. After waiting for a further 1 h, refreshing the sample with *p*-H$_2$, and repeating the SABRE process, a polarized signal for free Na^{15}NO$_2$ (δ_N 611.9) could also be detected and the observed signal for $\mathbf{5_A}$ increased in size. We therefore suspect that the reducing environment of this medium converts nitrate to nitrite in a metal-catalyzed reduction. To further probe this reduction, a sample containing [IrCl(COD)(IMes)] (20 mM), pyridine (3 equiv) and Na^{15}NO$_3$ (25 equiv) was exposed to 3 bar of H$_2$ at 298 K for 24 h and the growth of the hydride ligand resonance for $\mathbf{5_A}$ at δ_H −21.49 was monitored by thermally polarized ^{1}H NMR spectroscopy over the course of 24 h. The resulting integral data for this peak could be fitted to an exponential growth curve (see the Supporting Information). After 24 h and refreshing the H$_2$ atmosphere, further conversion to $\mathbf{5_A}$ could again be seen which indicates that H$_2$ is needed to drive this reaction. While the electrochemical reduction of nitrate is widely known[124,125] and limited examples of heterogeneous hydrogenative reduction of nitrate are also reported,[126−128] to the best of our knowledge the molecular reduction of nitrate using transition-metal catalysis has not received significant attention. Optimization of the phenomenon reported here may therefore provide a useful alternative.

CONCLUSIONS

In this work, we have demonstrated how the ^{15}N hyperpolarization of a range of important ^{15}N-synthons, including some which feature in the important nitrogen cycle (NO_2^- (28% polarization), NH_3 (3%), $PhCH_2NH_2$ (5%), NaN_3 (3%), and NO_3^- (0.1%)), is possible. When monitored by ^{15}N NMR, all these species yield strong signals that can be detected readily. The in-field, T_1 values of NO_2^- (17 s), ND_3 (36 s), $PhCH_2NH_2$ (12 s), and NaN_3 (50 s) mean that sufficient time exists to monitor their reactivity through hyperpolarized product responses. This has been demonstrated for the formation of phenyl diazonium, phenyl azide, a triazole, an amide, a sulfonamide, and two imines (Figure 4). In the case of phenyl azide formation, a pentazole intermediate was detected whose cyclic, rather than acyclic, formulation has been confirmed. Studies of the unlabeled formation of phenyl diazonium are also detailed.

Hence, these results demonstrate how SABRE reflects a versatile tool capable of tracking the preparation of a range of nitrogen rich products. We expect the future application of this approach to aid in achieving the optimized the synthesis of many materials, including important pharmaceuticals.

Furthermore, we demonstrate a biphasic method using a 15-crown-5 as a phase-transfer agent that yields >8% aqueous NO_2^- polarization. We expect this route to help SABRE deliver biocompatible products in the future as we expect it to produce large amounts of such hyperpolarized reagents in seconds. The recent report of 79% ^{15}N-derived SABRE hyperpolarization[62] suggests that with further optimization a currently unrivaled low-cost approach to rapidly deliver ^{15}N NMR sensitivity will therefore be obtained. Hence, the pioneering work of Bowers and Weitekamp again continues to expand beyond its original horizons.[129]

ASSOCIATED CONTENT

Supporting Information

The Supporting Information is available free of charge at https://pubs.acs.org/doi/10.1021/jacs.2c02619.

Full experimental methods, hyperpolarized NMR spectra, and characterization data (PDF)

AUTHOR INFORMATION

Corresponding Author

Simon B. Duckett − *Centre for Hyperpolarisation in Magnetic Resonance, Department of Chemistry, University of York, York YO10 5DD, U.K.*; orcid.org/0000-0002-9788-6615; Email: simon.duckett@york.ac.uk

Authors

Peter J. Rayner − *Centre for Hyperpolarisation in Magnetic Resonance, Department of Chemistry, University of York, York YO10 5DD, U.K.*; orcid.org/0000-0002-6577-4117

Marianna Fekete − *Centre for Hyperpolarisation in Magnetic Resonance, Department of Chemistry, University of York, York YO10 5DD, U.K.*

Callum A. Gater − *Centre for Hyperpolarisation in Magnetic Resonance, Department of Chemistry, University of York, York YO10 5DD, U.K.*; orcid.org/0000-0003-2457-0238

Fadi Ahwal − *Centre for Hyperpolarisation in Magnetic Resonance, Department of Chemistry, University of York, York YO10 5DD, U.K.*; orcid.org/0000-0002-5512-0275

Norman Turner − *Department of Engineering and Technology, University of Huddersfield, Huddersfield, West Yorkshire HD1 3DH, U.K.*

Aneurin J. Kennerley − *Centre for Hyperpolarisation in Magnetic Resonance, Department of Chemistry, University of York, York YO10 5DD, U.K.*

Complete contact information is available at: https://pubs.acs.org/10.1021/jacs.2c02619

Funding

S.B.D. and A.J.K. thank the following for supporting this work: The EPSRC (EP/R51181X/1, G0065601) and the University of York and Norman Turner (N0013902).

Notes

The authors declare no competing financial interest.

ACKNOWLEDGMENTS

We are grateful for the help from Dr. Victoria Annis.

ABBREVIATIONS

SABRE signal amplification by reversible exchange

p-H_2	*para*-hydrogen
PHIP	parahydrogen induced polarization
d-DNP	dissolution dynamic nuclear polarization
PET	positron emission tomography
DMAP	dimethylamino pyridine

REFERENCES

(1) Keshari, K. R.; Wilson, D. M. Chemistry and biochemistry of C-13 hyperpolarized magnetic resonance using dynamic nuclear polarization. *Chem. Soc. Rev.* **2014**, *43*, 1627−1659.

(2) Mugler, J. P.; Altes, T. A. Hyperpolarized 129Xe MRI of the human lung. *J. Magn. Reson. Imaging* **2013**, *37*, 313−331.

(3) Weitzberg, E.; Hezel, M.; Lundberg, J. O. Nitrate-Nitrite-Nitric Oxide Pathway: Implications for Anesthesiology and Intensive Care. *Anesthesiology* **2010**, *113*, 1460−1475.

(4) Adams, R. W.; Aguilar, J. A.; Atkinson, K. D.; Cowley, M. J.; Elliott, P. I.; Duckett, S. B.; Green, G. G.; Khazal, I. G.; López-Serrano, J.; Williamson, D. C. Reversible interactions with para-hydrogen enhance NMR sensitivity by polarization transfer. *Science* **2009**, *323*, 1708−1711.

(5) Reineri, F.; Boi, T.; Aime, S. ParaHydrogen Induced Polarization of C-13 carboxylate resonance in acetate and pyruvate. *Nat. Commun.* **2015**, *6*, 5858.

(6) Knecht, S.; Blanchard, J. W.; Barskiy, D.; Cavallari, E.; Dagys, L.; Dyke, E. V.; Tsukanov, M.; Bliemel, B.; Münnemann, K.; Aime, S.; Reineri, F.; Levitt, M. H.; Buntkowsky, G.; Pines, A.; Blümler, P.; Budker, D.; Eills, J. Rapid hyperpolarization and purification of the metabolite fumarate in aqueous solution. *Proc. Natl. Acad. Sci. U. S. A.* **2021**, *118*, No. e2025383118.

(7) Eills, J.; Cavallari, E.; Kircher, R.; Di Matteo, G.; Carrera, C.; Dagys, L.; Levitt, M. H.; Ivanov, K. L.; Aime, S.; Reineri, F.; Münnemann, K.; Budker, D.; Buntkowsky, G.; Knecht, S. Singlet-Contrast Magnetic Resonance Imaging: Unlocking Hyperpolarization with Metabolism**. *Angew. Chem., Int. Ed.* **2021**, *60*, 6791−6798.

(8) Blazina, D.; Duckett, S. B.; Dunne, J. P.; Godard, C. Applications of the parahydrogen phenomenon in inorganic chemistry. *Dalton Trans.* **2004**, 2601−2609.

(9) Shchepin, R. V.; Birchall, J. R.; Chukanov, N. V.; Kovtunov, K. V.; Koptyug, I. V.; Theis, T.; Warren, W. S.; Gelovani, J. G.; Goodson, B. M.; Shokouhi, S.; Rosen, M. S.; Yen, Y. F.; Pham, W.; Chekmenev, E. Y. Hyperpolarizing Concentrated Metronidazole (NO2)-N-15 Group over Six Chemical Bonds with More than 15% Polarization and a 20 Minute Lifetime. *Chem. − Eur. J.* **2019**, *25*, 8829−8836.

(10) Shchepin, R. V.; Barskiy, D. A.; Coffey, A. M.; Feldman, M. A.; Kovtunova, L. M.; Bukhtiyarov, V. I.; Kovtunov, K. V.; Goodson, B. M.; Koptyug, I. V.; Chekmenev, E. Y. Robust Imidazole-N-15(2) Synthesis for High-Resolution Low-Field (0.05 T) (15)NHyperpolarized NMR Spectroscopy. *ChemistrySelect* **2017**, *2*, 4478−4483.

(11) Hövener, J.-B.; Pravdivtsev, A. N.; Kidd, B.; Bowers, C. R.; Glöggler, S.; Kovtunov, K. V.; Plaumann, M.; Katz-Brull, R.; Buckenmaier, K.; Jerschow, A.; Reineri, F.; Theis, T.; Shchepin, R. V.; Wagner, S.; Bhattacharya, P.; Zacharias, N. M.; Chekmenev, E. Y. Parahydrogen-Based Hyperpolarization for Biomedicine. *Angew. Chem., Int. Ed.* **2018**, *57*, 11140−11162.

(12) Ko, Y.; Bonner, F. T.; Crull, G. B.; Harbison, G. S. Protonation nitrogen shielding and NOE in aqueous nitrite and solid-state nitrogen-15 NMR of nitrosyl and nitryl tetrafluoroborate. *Inorg. Chem.* **1993**, *32*, 3316−3319.

(13) Thorn, K. A.; Mikita, M. A. Nitrite Fixation by Humic Substances Nitrogen-15 Nuclear Magnetic Resonance Evidence for Potential Intermediates in Chemodenitrification. *Soil Sci. Soc. Am. J.* **2000**, *64*, 568−582.

(14) Sakhaei, Z.; Kundu, S.; Donnelly, J. M.; Bertke, J. A.; Kim, W. Y.; Warren, T. H. Nitric oxide release via oxygen atom transfer from nitrite at copper(ii). *Chem. Commun.* **2017**, *53*, 549−552.

(15) Gamliel, A.; Uppala, S.; Sapir, G.; Harris, T.; Nardi-Schreiber, A.; Shaul, D.; Sosna, J.; Gomori, J. M.; Katz-Brull, R. Hyperpolarized [15N]nitrate as a potential long lived hyperpolarized contrast agent for MRI. *J. Magn. Reson.* **2019**, *299*, 188−195.

(16) Godard, C.; Lopez-Serrano, J.; Galvez-Lopez, M. D.; Rosello-Merino, M.; Duckett, S. B.; Khazal, I.; Lledos, A.; Whitwood, A. C. Detection of platinum dihydride bisphosphine complexes and studies of their reactivity through para-hydrogen-enhanced NMR methods. *Magn. Reson. Chem.* **2008**, *46*, S107−S114.

(17) Vazquez-Serrano, L. D.; Owens, B. T.; Buriak, J. M. Catalytic olefin hydrogenation using N-heterocyclic carbene-phosphine complexes of iridium. *Chem. Commun.* **2002**, *21*, 2518−2519.

(18) Giernoth, R.; Heinrich, H.; Adams, N. J.; Deeth, R. J.; Bargon, J.; Brown, J. M. PHIP detection of a transient rhodium dihydride intermediate in the homogeneous hydrogenation of dehydroamino acids. *J. Am. Chem. Soc.* **2000**, *122*, 12381−12382.

(19) Torres, O.; Procacci, B.; Halse, M. E.; Adams, R. W.; Blazina, D.; Duckett, S. B.; Eguillor, B.; Green, R. A.; Perutz, R. N.; Williamson, D. C. Photochemical Pump and NMR Probe: Chemically Created NMR Coherence on a Microsecond Time Scale. *J. Am. Chem. Soc.* **2014**, *136*, 10124−10131.

(20) Delwiche, C. C. The Nitrogen Cycle. *Sci. Am.* **1970**, *223*, 136−146.

(21) Cammack, R.; Joannou, C. L.; Cui, X.-Y.; Torres Martinez, C.; Maraj, S. R.; Hughes, M. N. Nitrite and nitrosyl compounds in food preservation. *Biochim. Biophys. Acta, Bioenerg.* **1999**, *1411*, 475−488.

(22) Shiva, S. Nitrite: A physiological store of nitric oxide and modulator of mitochondrial function. *Redox Biol.* **2013**, *1*, 40−44.

(23) Chui, J. S. W.; Poon, W. T.; Chan, K. C.; Chan, A. Y. W.; Buckley, T. A. Nitrite-induced methaemoglobinaemia − aetiology, diagnosis and treatment. *Anaesthesia* **2005**, *60*, 496−500.

(24) EFSA Panel on Food Additives and Nutrient Sources added to Food (ANS); Mortensen, A.; Aguilar, F.; Crebelli, R.; Di Domenico, A.; Dusemund, B.; Frutos, M. J.; Galtier, P.; Gott, D.; Gundert-Remy, U.; Lambré, C.; Leblanc, J.-C.; Lindtner, O.; Moldeus, P.; Mosesso, P.; Oskarsson, A.; Parent-Massin, D.; Stankovic, I.; Waalkens-Berendsen, I.; Woutersen, R. A.; Wright, M.; van den Brandt, P.; Fortes, C.; Merino, L.; Toldrà, F.; Arcella, D.; Christodoulidou, A.; Cortinas Abrahantes, J.; Barrucci, F.; Garcia, A.; Pizzo, F.; Battacchi, D.; Younes, M. Re-evaluation of potassium nitrite (E 249) and sodium nitrite (E 250) as food additives. *EFSA J.* **2017**, *15*, No. e04786.

(25) Walker, R. Nitrates, nitrites and N-nitrosocompounds: A review of the occurrence in food and diet and the toxicological implications. *Food Addit. Contam.* **1990**, *7*, 717−768.

(26) Bebarta, V. S.; Brittain, M.; Chan, A.; Garrett, N.; Yoon, D.; Burney, T.; Mukai, D.; Babin, M.; Pilz, R. B.; Mahon, S. B.; Brenner, M.; Boss, G. R. Sodium Nitrite and Sodium Thiosulfate Are Effective Against Acute Cyanide Poisoning When Administered by Intramuscular Injection. *Ann. Emerg. Med.* **2017**, *69*, 718−725.e4.

(27) Mukhopadhyay, S.; Batra, S. Applications of Sodium Nitrite in Organic Synthesis. *Eur. J. Org. Chem.* **2019**, *2019*, 6424−6451.

(28) Halfen, J. A.; Mahapatra, S.; Wilkinson, E. C.; Gengenbach, A. J.; Young, V. G.; Que, L.; Tolman, W. B. Synthetic Modeling of Nitrite Binding and Activation by Reduced Copper Proteins. Characterization of Copper(I)−Nitrite Complexes That Evolve Nitric Oxide. *J. Am. Chem. Soc.* **1996**, *118*, 763−776.

(29) Timmons, A. J.; Symes, M. D. Converting between the oxides of nitrogen using metal−ligand coordination complexes. *Chem. Soc. Rev.* **2015**, *44*, 6708−6722.

(30) Takeuchi, A.; Sato, K.; Sone, K.; Yamada, S.; Yamasaki, K. Preparation of some nitro-amine complexes of nickel and their properties. *Inorg. Chim. Acta* **1967**, *1*, 399−402.

(31) Goodgame, D. M. L.; Hitchman, M. A. Studies of Nitro and Nitrito Complexes. I. Some Nitrito Complexes of Nickel(II). *Inorg. Chem.* **1964**, *3*, 1389−1394.

(32) Goodgame, D. M. L.; Hitchman, M. A. Studies of Nitro and Nitrito Complexes. III. Some Nitro Complexes of Nickel(II) and a Nitro-Nitrito Equilibrium. *Inorg. Chem.* **1966**, *5*, 1303−1307.

(33) Gwak, J.; Ahn, S.; Baik, M.-H.; Lee, Y. One metal is enough: a nickel complex reduces nitrate anions to nitrogen gas. *Chem. Sci.* **2019**, *10*, 4767−4774.

https://doi.org/10.1021/jacs.2c02619
J. Am. Chem. Soc. 2022, 144, 8756−8769

(34) Nakamura, I.; Funasako, Y.; Mochida, T. Nitro−Nitrito Photoisomerization of Platinum(II) Complexes with Pt(NO2)42− and (FSO2)2N− Anions: Correlation between Isomerization Ratio and Reaction Cavity. *Cryst. Growth Des.* **2020**, *20*, 8047−8052.
(35) Badar Ud, D.; Bailar, J. C. Observations on the oxidation and reduction of platinum(II) nitro complexes. *J. Inorg. Nucl.* **1961**, *22*, 241−245.
(36) Gel'fman, M. I.; Starkina, N. A.; Salishcheva, O. V.; Moldagulova, N. E. Trans-influence of a nitro group in platinum complexes. *Russ. J. Inorg. Chem.* **2007**, *52*, 1551−1556.
(37) Rayner, P. J.; Duckett, S. Signal Amplification by Reversible Exchange (SABRE): From Discovery to Diagnosis. *Angew. Chem., Int. Ed.* **2018**, *57*, 6742−6753.
(38) Kovtunov, K. V.; Pokochueva, E. V.; Salnikov, O. G.; Cousin, S. F.; Kurzbach, D.; Vuichoud, B.; Jannin, S.; Chekmenev, E. Y.; Goodson, B. M.; Barskiy, D. A.; Koptyug, I. V. Hyperpolarized NMR Spectroscopy: d-DNP, PHIP, and SABRE Techniques. *Chem. − Asian J.* **2018**, *13*, 1857−1871.
(39) Tickner, B. J.; Semenova, O.; Iali, W.; Rayner, P. J.; Whitwood, A. C.; Duckett, S. B. Optimisation of pyruvate hyperpolarisation using SABRE by tuning the active magnetisation transfer catalyst. *Catal. Sci. Technol.* **2020**, *10*, 1343−1355.
(40) Iali, W.; Roy, S. S.; Tickner, B. J.; Ahwal, F.; Kennerley, A. J.; Duckett, S. B. Hyperpolarising Pyruvate through Signal Amplification by Reversible Exchange (SABRE). *Angew. Chem., Int. Ed.* **2019**, *58*, 10271−10275.
(41) Gemeinhardt, M.; Limbach, M.; Gebhardt, T.; Eriksson, C.; Eriksson, S.; Lindale, J.; Goodson, E.; Warren, W.; Chekmenev, E.; Goodson, B. "Direct" 13C Hyperpolarization of 13C-Acetate by MicroTesla NMR Signal Amplification by Reversible Exchange (SABRE). *Angew. Chem., Int. Ed.* **2020**, *59*, 418−423.
(42) Rayner, P. J.; Burns, M. J.; Olaru, A. M.; Norcott, P.; Fekete, M.; Green, G. G. R.; Highton, L. A. R.; Mewis, R. E.; Duckett, S. B. Delivering strong 1H nuclear hyperpolarization levels and long magnetic lifetimes through signal amplification by reversible exchange. *Proc. Natl. Acad. Sci. U. S. A.* **2017**, *114*, E3188−E3194.
(43) Adams, R. W.; Duckett, S. B.; Green, R. A.; Williamson, D. C.; Green, G. G. R. A theoretical basis for spontaneous polarization transfer in non-hydrogenative parahydrogen-induced polarization. *Chem. Phys.* **2009**, *131*, 194505.
(44) Barskiy, D. A.; Pravdivtsev, A. N.; Ivanov, K. L.; Kovtunov, K. V.; Koptyug, I. V. A simple analytical model for signal amplification by reversible exchange (SABRE) process. *Phys. Chem. Chem. Phys.* **2016**, *18*, 89−93.
(45) Knecht, S.; Pravdivtsev, A. N.; Hovener, J.-B.; Yurkovskaya, A. V.; Ivanov, K. L. Quantitative description of the SABRE process: rigorous consideration of spin dynamics and chemical exchange. *RSC Adv.* **2016**, *6*, 24470−24477.
(46) Pravdivtsev, A. N.; Yurkovskaya, A. V.; Vieth, H.-M.; Ivanov, K. L.; Kaptein, R. Level Anti-Crossings are a Key Factor for Understanding para-Hydrogen-Induced Hyperpolarization in SABRE Experiments. *ChemPhysChem* **2013**, *14*, 3327−3331.
(47) Pravdivtsev, A. N.; Ivanov, K. L.; Yurkovskaya, A. V.; Petrov, P. A.; Limbach, H. H.; Kaptein, R.; Vieth, H. M. Spin polarization transfer mechanisms of SABRE: A magnetic field dependent study. *J. Magn. Reson.* **2015**, *261*, 73−82.
(48) Theis, T.; Truong, M.; Coffey, A. M.; Chekmenev, E. Y.; Warren, W. S. LIGHT-SABRE enables efficient in-magnet catalytic hyperpolarization. *J. Magn. Reson.* **2014**, *248*, 23−26.
(49) Barskiy, D. A.; Shchepin, R. V.; Tanner, C. P. N.; Colell, J. F. P.; Goodson, B. M.; Theis, T.; Warren, W. S.; Chekmenev, E. Y. The Absence of Quadrupolar Nuclei Facilitates Efficient 13C Hyperpolarization via Reversible Exchange with Parahydrogen. *ChemPhysChem* **2017**, *18*, 1493−1498.
(50) Zhou, Z.; Yu, J.; Colell, J. F. P.; Laasner, R.; Logan, A.; Barskiy, D. A.; Shchepin, R. V.; Chekmenev, E. Y.; Blum, V.; Warren, W. S.; Theis, T. Long-Lived 13C2 Nuclear Spin States Hyperpolarized by Parahydrogen in Reversible Exchange at Microtesla Fields. *J. Phys. Chem. Lett.* **2017**, *8*, 3008−3014.
(51) Theis, T.; Truong, M. L.; Coffey, A. M.; Shchepin, R. V.; Waddell, K. W.; Shi, F.; Goodson, B. M.; Warren, W. S.; Chekmenev, E. Y. Microtesla SABRE Enables 10% Nitrogen-15 Nuclear Spin Polarization. *J. Am. Chem. Soc.* **2015**, *137*, 1404−1407.
(52) Roy, S. S.; Rayner, P. J.; Burns, M. J.; Duckett, S. B. A simple and cost-efficient technique to generate hyperpolarized long-lived 15N-15N nuclear spin order in a diazine by signal amplification by reversible exchange. *J. Chem. Phys.* **2020**, *152*, No. 014201.
(53) Shchepin, R. V.; Barskiy, D. A.; Mikhaylov, D. M.; Chekmenev, E. Y. Efficient Synthesis of Nicotinamide-1-15N for Ultrafast NMR Hyperpolarization Using Parahydrogen. *Bioconjugate Chem.* **2016**, *27*, 878−882.
(54) Theis, T.; Ortiz, G. X.; Logan, A. W. J.; Claytor, K. E.; Feng, Y.; Huhn, W. P.; Blum, V.; Malcolmson, S. J.; Chekmenev, E. Y.; Wang, Q.; Warren, W. S. Direct and cost-efficient hyperpolarization of long-lived nuclear spin states on universal $^{15}N_2$−diazirine molecular tags. *Sci. Adv.* **2016**, *2*, No. e1501438.
(55) Barskiy, D. A.; Shchepin, R. V.; Coffey, A. M.; Theis, T.; Warren, W. S.; Goodson, B. M.; Chekmenev, E. Y. Over 20% 15N Hyperpolarization in Under One Minute for Metronidazole, an Antibiotic and Hypoxia Probe. *J. Am. Chem. Soc.* **2016**, *138*, 8080−8083.
(56) Truong, M. L.; Theis, T.; Coffey, A. M.; Shchepin, R. V.; Waddell, K. W.; Shi, F.; Goodson, B. M.; Warren, W. S.; Chekmenev, E. Y. 15N Hyperpolarization by Reversible Exchange Using SABRE-SHEATH. *J. Phys. Chem. C* **2015**, *119*, 8786−8797.
(57) Zhivonitko, V. V.; Skovpin, I. V.; Koptyug, I. V. Strong ^{31}P nuclear spin hyperpolarization produced via reversible chemical interaction with parahydrogen. *Chem. Commun.* **2015**, *51*, 2506−2509.
(58) Burns, M. J.; Rayner, P. J.; Green, G. G. R.; Highton, L. A. R.; Mewis, R. E.; Duckett, S. B. Improving the Hyperpolarization of 31P Nuclei by Synthetic Design. *J. Phys. Chem. B* **2015**, *119*, 5020−5027.
(59) Olaru, A. M.; Burt, A.; Rayner, P. J.; Hart, S. J.; Whitwood, A. C.; Green, G. G. R.; Duckett, S. B. Using signal amplification by reversible exchange (SABRE) to hyperpolarise 119Sn and 29Si NMR nuclei. *Chem. Commun.* **2016**, *52*, 14482−14485.
(60) Rayner, P. J.; Norcott, P.; Appleby, K. M.; Iali, W.; John, R. O.; Hart, S. J.; Whitwood, A. C.; Duckett, S. B. Fine-tuning the efficiency of para-hydrogen-induced hyperpolarization by rational N-heterocyclic carbene design. *Nat. Commun.* **2018**, *9*, 4251.
(61) Cowley, M. J.; Adams, R. W.; Atkinson, K. D.; Cockett, M. C. R.; Duckett, S. B.; Green, G. G. R.; Lohman, J. A. B.; Kerssebaum, R.; Kilgour, D.; Mewis, R. E. Iridium N-Heterocyclic Carbene Complexes as Efficient Catalysts for Magnetization Transfer from para-Hydrogen. *J. Am. Chem. Soc.* **2011**, *133*, 6134−6137.
(62) Fekete, M.; Ahwal, F.; Duckett, S. B. Remarkable Levels of N-15 Polarization Delivered through SABRE into Unlabeled Pyridine, Pyrazine, or Metronidazole Enable Single Scan NMR Quantification at the mM Level. *J. Phys. Chem. B* **2020**, *124*, 4573−4580.
(63) Svyatova, A.; Skovpin, I. V.; Chukanov, N. V.; Kovtunov, K. V.; Chekmenev, E. Y.; Pravdivtsev, A. N.; Hovener, J. B.; Koptyug, I. V. N-15 MRI of SLIC-SABRE Hyperpolarized N-15-Labelled Pyridine and Nicotinamide. *Chem. − Eur. J.* **2019**, *25*, 8465−8470.
(64) Pravdivtsev, A. N.; Yurkovskaya, A. V.; Zimmermann, H.; Vieth, H. M.; Ivanov, K. L. Enhancing NMR of insensitive nuclei by transfer of SABRE spin hyperpolarization. *Chem. Phys. Lett.* **2016**, *661*, 77−82.
(65) Kidd, B. E.; Gesiorski, J. L.; Gemeinhardt, M. E.; Shchepin, R. V.; Kovtunov, K. V.; Koptyug, I. V.; Chekmenev, E. Y.; Goodson, B. M. Facile Removal of Homogeneous SABRE Catalysts for Purifying Hyperpolarized Metronidazole, a Potential Hypoxia Sensor. *J. Phys. Chem. C* **2018**, *122*, 16848−16852.
(66) Skovpin, I. V.; Svyatova, A.; Chukanov, N.; Chekmenev, E. Y.; Kovtunov, K. V.; Koptyug, I. V. N-15 Hyperpolarization of Dalfampridine at Natural Abundance for Magnetic Resonance Imaging. *Chem. − Eur. J.* **2019**, *25*, 12694−12697.
(67) Eshuis, N.; van Weerdenburg, B. J. A.; Feiters, M. C.; Rutjes, F. P. J. T.; Wijmenga, S. S.; Tessari, M. Quantitative Trace Analysis of Complex Mixtures Using SABRE Hyperpolarization. *Angew. Chem., Int. Ed.* **2015**, *54*, 1481−1484.

https://doi.org/10.1021/jacs.2c02619
J. Am. Chem. Soc. 2022, 144, 8756−8769

(68) van Weerdenburg, B. J. A.; Gloeggler, S.; Eshuis, N.; Engwerda, A. H. J.; Smits, J. M. M.; de Gelder, R.; Appelt, S.; Wymenga, S. S.; Tessari, M.; Feiters, M. C.; Blumich, B.; Rutjes, F. P. J. T. Ligand effects of NHC-iridium catalysts for signal amplification by reversible exchange (SABRE). *Chem. Commun.* **2013**, *49*, 7388−7390.
(69) Levitt, M. H.; Singlet, N. M. R. *Annu. Rev. Phys. Chem.* **2012**, 89−105.
(70) Roy, S. S.; Norcott, P.; Rayner, P. J.; Green, G. G. R.; Duckett, S. B. A Hyperpolarizable 1H Magnetic Resonance Probe for Signal Detection 15 Minutes after Spin Polarization Storage. *Angew. Chem., Int. Ed.* **2016**, *55*, 15642−15645.
(71) Roy, S. S.; Norcott, P.; Rayner, P. J.; Green, G. G. R.; Duckett, S. B. A Simple Route to Strong Carbon-13 NMR Signals Detectable for Several Minutes. *Chem. − Eur. J.* **2017**, *23*, 10496−10500.
(72) Zhang, G. N.; Colell, J. F. P.; Glachet, T.; Lindale, J. R.; Reboul, V.; Theis, T.; Warren, W. S. Terminal Diazirines Enable Reverse Polarization Transfer from N-15(2) Singlets. *Angew. Chem., Int. Ed.* **2019**, *58*, 11118−11124.
(73) Shen, K.; Logan, A. W. J.; Colell, J. F. P.; Bae, J.; Ortiz, G. X., Jr.; Theis, T.; Warren, W. S.; Malcolmson, S. J.; Wang, Q. Diazirines as Potential Molecular Imaging Tags: Probing the Requirements for Efficient and Long-Lived SABRE-Induced Hyperpolarization. *Angew. Chem., Int. Ed.* **2017**, *56*, 12112−12116.
(74) Procacci, B.; Roy, S. S.; Norcott, P.; Turner, N.; Duckett, S. B. Unlocking a Diazirine Long-Lived Nuclear Singlet State via Photochemistry: NMR Detection and Lifetime of an Unstabilized Diazo-Compound. *J. Am. Chem. Soc.* **2018**, *140*, 16855−16864.
(75) Norcott, P.; Burns, M. J.; Rayner, P. J.; Mewis, R. E.; Duckett, S. B. Using 2H Labelling to Improve the NMR Detectability of Pyridine and its Derivatives by SABRE. *Magn. Reson. Chem.* **2018**, 663.
(76) Norcott, P.; Rayner, P. J.; Green, G. G. R.; Duckett, S. Achieving High 1H Nuclear Hyperpolarization Levels with Long Lifetimes in a Range of Tuberculosis Drug Scaffolds. *Chem. − Eur. J.* **2017**, *23*, 16990−16997.
(77) Fekete, M.; Bayfield, O.; Duckett, S. B.; Hart, S.; Mewis, R. E.; Pridmore, N.; Rayner, P. J.; Whitwood, A. Iridium(III) Hydrido N-Heterocyclic Carbene−Phosphine Complexes as Catalysts in Magnetization Transfer Reactions. *Inorg. Chem.* **2013**, *52*, 13453−13461.
(78) Lloyd, L. S.; Asghar, A.; Burns, M. J.; Charlton, A.; Coombes, S.; Cowley, M. J.; Dear, G. J.; Duckett, S. B.; Genov, G. R.; Green, G. G. R.; Highton, L. A. R.; Hooper, A. J. J.; Khan, M.; Khazal, I. G.; Lewis, R. J.; Mewis, R. E.; Roberts, A. D.; Ruddlesden, A. J. Hyperpolarisation through reversible interactions with parahydrogen. *Catal. Sci. Technol.* **2014**, *4*, 3544−3554.
(79) Rayner, P. J.; Gillions, J. P.; Hannibal, V. D.; John, R. O.; Duckett, S. B. Hyperpolarisation of weakly binding N-heterocycles using signal amplification by reversible exchange. *Chem. Sci.* **2021**, *12*, 5910−5917.
(80) Rayner, P. J.; Tickner, B. J.; Iali, W.; Fekete, M.; Robinson, A. D.; Duckett, S. B. Relayed hyperpolarization from para-hydrogen improves the NMR detectability of alcohols. *Chem. Sci.* **2019**, *10*, 7709−7717.
(81) Iali, W.; Rayner, P. J.; Duckett, S. B. Using parahydrogen to hyperpolarize amines, amides, carboxylic acids, alcohols, phosphates, and carbonates. *Sci. Adv.* **2018**, *4*, No. eaao6250.
(82) Shchepin, R. V.; Truong, M. L.; Theis, T.; Coffey, A. M.; Shi, F.; Waddell, K. W.; Warren, W. S.; Goodson, B. M.; Chekmenev, E. Y. Hyperpolarization of "Neat" Liquids by NMR Signal Amplification by Reversible Exchange. *J. Phys. Chem. Lett.* **2015**, *6*, 1961−1967.
(83) Colell, J.; Logan, A. W. J.; Zhou, Z.; Lindale, J. R.; Laasner, R.; Shchepin, R.; Chekmenev, E.; Blum, V.; Warren, W. S.; Malcolmson, S. J.; Theis, T. Rational ligand choice extends the SABRE substrate scope. *Chem. Commun.* **2020**, *56*, 9336−9339.
(84) Iali, W.; Rayner, P. J.; Alshehri, A.; Holmes, A. J.; Ruddlesden, A. J.; Duckett, S. B. Direct and indirect hyperpolarisation of amines using parahydrogen. *Chem. Sci.* **2018**, *9*, 3677−3684.
(85) Rayner, P. J.; Richardson, P. M.; Duckett, S. B. The Detection and Reactivity of Silanols and Silanes Using Hyperpolarized 29Si Nuclear Magnetic Resonance. *Angew. Chem., Int. Ed.* **2020**, *59*, 2710−2714.
(86) Richardson, P. M.; Iali, W.; Roy, S. S.; Rayner, P. J.; Halse, M. E.; Duckett, S. B. Rapid 13C NMR hyperpolarization delivered from para-hydrogen enables the low concentration detection and quantification of sugars. *Chem. Sci.* **2019**, *10*, 10607−10619.
(87) Tickner, B. J.; Lewis, J. S.; John, R. O.; Whitwood, A. C.; Duckett, S. B. Mechanistic insight into novel sulfoxide containing SABRE polarisation transfer catalysts. *Dalton Trans.* **2019**, *48*, 15198−15206.
(88) Mewis, R. E.; Green, R. A.; Cockett, M. C. R.; Cowley, M. J.; Duckett, S. B.; Green, G. G. R.; John, R. O.; Rayner, P. J.; Williamson, D. C. Strategies for the Hyperpolarization of Acetonitrile and Related Ligands by SABRE. *J. Phys. Chem. B* **2015**, *119*, 1416−1424.
(89) Bagley, M. C.; Alnomsy, A.; Sharhan, H. I. Rapid Protium−Deuterium Exchange of 4-Aminopyridines in Neutral D2O under Microwave Irradiation. *Synlett* **2016**, *27*, 2467−2472.
(90) van Weerdenburg, B. J. A.; Eshuis, N.; Tessari, M.; Rutjes, F. P. J. T.; Feiters, M. C. Application of the [small pi]-accepting ability parameter of N-heterocyclic carbene ligands in iridium complexes for signal amplification by reversible exchange (SABRE). *Dalton Trans.* **2015**, *44*, 15387−15390.
(91) Poater, A.; Cosenza, B.; Correa, A.; Giudice, S.; Ragone, F.; Scarano, V.; Cavallo, L. SambVca: A Web Application for the Calculation of the Buried Volume of N-Heterocyclic Carbene Ligands. *Eur. J. Inorg. Chem.* **2009**, *2009*, 1759−1766.
(92) Zhang, Y.; Lavigne, G.; Lugan, N.; César, V. Buttressing Effect as a Key Design Principle towards Highly Efficient Palladium/N-Heterocyclic Carbene Buchwald−Hartwig Amination Catalysts. *Chem. − Eur. J.* **2017**, *23*, 13792−13801.
(93) Zhang, Y.; César, V.; Storch, G.; Lugan, N.; Lavigne, G. Skeleton Decoration of NHCs by Amino Groups and its Sequential Booster Effect on the Palladium-Catalyzed Buchwald−Hartwig Amination. *Angew. Chem., Int. Ed.* **2014**, *53*, 6482−6486.
(94) Izatt, R. M.; Bradshaw, J. S.; Nielsen, S. A.; Lamb, J. D.; Christensen, J. J.; Sen, D. Thermodynamic and kinetic data for cation-macrocycle interaction. *Chem. Rev.* **1985**, *85*, 271−339.
(95) More, M. B.; Ray, D.; Armentrout, P. B. Intrinsic Affinities of Alkali Cations for 15-Crown-5 and 18-Crown-6: Bond Dissociation Energies of Gas-Phase M+−Crown Ether Complexes. *J. Am. Chem. Soc.* **1999**, *121*, 417−423.
(96) Mewis, R. E.; Atkinson, K. D.; Cowley, M. J.; Duckett, S. B.; Green, G. G. R.; Green, R. A.; Highton, L. A. R.; Kilgour, D.; Lloyd, L. S.; Lohman, J. A. B.; Williamson, D. C. Probing signal amplification by reversible exchange using an NMR flow system. *Magn. Reson. Chem.* **2014**, *52*, 358−369.
(97) Colell, J. F. P.; Logan, A. W. J.; Zhou, Z.; Shchepin, R. V.; Barskiy, D. A.; Ortiz, G. X.; Wang, Q.; Malcolmson, S. J.; Chekmenev, E. Y.; Warren, W. S.; Theis, T. Generalizing, Extending, and Maximizing Nitrogen-15 Hyperpolarization Induced by Parahydrogen in Reversible Exchange. *J. Phys. Chem. C* **2017**, *121*, 6626−6634.
(98) Zhang, G.; Colell, J. F. P.; Glachet, T.; Lindale, J. R.; Reboul, V.; Theis, T.; Warren, W. S. Terminal Diazirines Enable Reverse Polarization Transfer from 15N2 Singlets. *Angew. Chem., Int. Ed.* **2019**, *58*, 11118−11124.
(99) Hodgson, H. H. The Sandmeyer Reaction. *Chem. Rev.* **1947**, *40*, 251−277.
(100) Sandmeyer, T. Ueber die Ersetzung der Amidgruppe durch Chlor in den aromatischen Substanzen. *Ber. Dtsch. Chem. Ges.* **1884**, *17*, 1633−1635.
(101) Mo, F.; Qiu, D.; Zhang, Y.; Wang, J. Renaissance of Sandmeyer-Type Reactions: Conversion of Aromatic C−N Bonds into C−X Bonds (X = B, Sn, P, or CF3). *Acc. Chem. Res.* **2018**, *51*, 496−506.
(102) Leas, D. A.; Dong, Y.; Vennerstrom, J. L.; Stack, D. E. One-Pot, Metal-Free Conversion of Anilines to Aryl Bromides and Iodides. *Org. Lett.* **2017**, *19*, 2518−2521.
(103) Liu, Q.; Sun, B.; Liu, Z.; Kao, Y.; Dong, B.-W.; Jiang, S.-D.; Li, F.; Liu, G.; Yang, Y.; Mo, F. A general electrochemical strategy for the Sandmeyer reaction. *Chem. Sci.* **2018**, *9*, 8731−8737.
(104) Zhong, T.; Pang, M.-K.; Chen, Z.-D.; Zhang, B.; Weng, J.; Lu, G. Copper-free Sandmeyer-type Reaction for the Synthesis of Sulfonyl Fluorides. *Org. Lett.* **2020**, *22*, 3072−3078.

https://doi.org/10.1021/jacs.2c02619
J. Am. Chem. Soc. 2022, 144, 8756−8769

(105) Olah, G. A.; Herges, R.; Laali, K.; Segal, G. A. Onium ions. 34. The methoxydiazonium ion: preparation, proton, carbon-13, and nitrogen-15 NMR and IR structural studies, theoretical calculations, and reaction with aromatics. Attempted preparation and the intermediacy of the hydroxydiazonium ion. *J. Am. Chem. Soc.* **1986**, *108*, 2054−2057.
(106) Elofson, R. M.; Cyr, N.; Laidler, J. K.; Schulz, K. F.; Gadallah, F. F. Correlation of 13C and 15N nuclear magnetic resonance chemical shifts with polarographic reduction potentials of para-substituted benzenediazonium salts and their electronic structures. *Can. J. Chem.* **1984**, *62*, 92−95.
(107) Barraclough, R.; Jones, F.; Patterson, D.; Tetlow, A. The Photochemical Decomposition of Aryldiazonium Salts I—Stability and Quantum Yields. *J. Soc. Dyers Colour.* **1972**, *88*, 22−25.
(108) Mo, F.; Dong, G.; Zhang, Y.; Wang, J. Recent applications of arene diazonium salts in organic synthesis. *Org. Biomol.* **2013**, *11*, 1582−1593.
(109) Ritchie, C. D.; Wright, D. J. Anion-cation combination reactions. III. Reaction of diazonium ions with azide ion in aqueous solution. *J. Am. Chem. Soc.* **1971**, *93*, 2429−2432.
(110) Butler, R. N.; Fox, A.; Collier, S.; Burke, L. A. Pentazole chemistry: the mechanism of the reaction of aryldiazonium chlorides with azide ion at −80 °C: concerted versus stepwise formation of arylpentazoles, detection of a pentazene intermediate, a combined 1H and 15N NMR experimental and ab initio theoretical study. *J. Chem. Soc., Perkin Trans. 2* **1998**, 2243−2248.
(111) Joshi, S. M.; de Cózar, A.; Gómez-Vallejo, V.; Koziorowski, J.; Llop, J.; Cossío, F. P. Synthesis of radiolabelled aryl azides from diazonium salts: experimental and computational results permit the identification of the preferred mechanism. *Chem. Commun.* **2015**, *51*, 8954−8957.
(112) Dommerholt, J.; Schmidt, S.; Temming, R.; Hendriks, L. J. A.; Rutjes, F. P. J. T.; van Hest, J. C. M.; Lefeber, D. J.; Friedl, P.; van Delft, F. L. Readily Accessible Bicyclononynes for Bioorthogonal Labeling and Three-Dimensional Imaging of Living Cells. *Angew. Chem., Int. Ed.* **2010**, *49*, 9422−9425.
(113) Kim, E.; Koo, H. Biomedical applications of copper-free click chemistry: in vitro, in vivo, and ex vivo. *Chem. Sci.* **2019**, *10*, 7835−7851.
(114) Jewett, J. C.; Bertozzi, C. R. Cu-free click cycloaddition reactions in chemical biology. *Chem. Soc. Rev.* **2010**, *39*, 1272−1279.
(115) Vaneeckhaute, E.; De Ridder, S.; Tyburn, J.-M.; Kempf, J. G.; Taulelle, F.; Martens, J. A.; Breynaert, E. Long-Term Generation of Longitudinal Spin Order Controlled by Ammonia Ligation Enables Rapid SABRE Hyperpolarized 2D NMR. *ChemPhysChem* **2021**, *22*, 1170−1177.
(116) Iali, W.; Olaru, A. M.; Green, G. G. R.; Duckett, S. B. Achieving High Levels of NMR-Hyperpolarization in Aqueous Media With Minimal Catalyst Contamination Using SABRE. *Chem. − Eur. J.* **2017**, *23*, 10491−10495.
(117) Manoharan, A.; Rayner, P. J.; Iali, W.; Burns, M. J.; Perry, V. H.; Duckett, S. B. Achieving Biocompatible SABRE: An in vitro Cytotoxicity Study. *ChemMedChem* **2018**, *13*, 352−359.
(118) Landini, D.; Maia, A.; Montanari, F.; Pirisi, F. M. Crown ethers as phase-transfer catalysts. A comparison of anionic activation in aqueous−organic two-phase systems and in low polarity anhydrous solutions by perhydrodibenzo-18-crown-6, lipophilic quaternary salts, and cryptands. *J. Chem. Soc., Perkin Trans. 2* **1980**, *1*, 46−51.
(119) Krushna, C.; Mohapatra, C.; Dash, K. C. 4-, 5- and 6-coordinate complexes of copper(II) with substituted imidazoles. *J. Inorg. Nucl.* **1977**, *39*, 1253−1258.
(120) Mu, J.; Perlmutter, D. D. Thermal decomposition of metal nitrates and their hydrates. *Thermochim. Acta* **1982**, *56*, 253−260.
(121) Dollimore, D.; Gamlen, G. A.; Taylor, T. J. Degradation studies on nickel nitrate hexahydrate: Part 2. evolved gas analysis. *Thermochim. Acta* **1985**, *91*, 287−297.
(122) Dollimore, D.; Gamlen, G. A.; Taylor, T. J. Degradation studies on nickel nitrate hexahydrate. Part 1. Effect of experimental conditions. *Thermochim. Acta* **1985**, *86*, 119−132.
(123) Wheeler, M. T.; Walmsley, F. Transition metal nitrate complexes of 1,4,5-triazanaphthalene. *Thermochim. Acta* **1986**, *108*, 325−336.
(124) Lu, X.; Song, H.; Cai, J.; Lu, S. Recent development of electrochemical nitrate reduction to ammonia: A mini review. *Electrochem. Commun.* **2021**, *129*, No. 107094.
(125) Wang, Y.; Wang, C.; Li, M.; Yu, Y.; Zhang, B. Nitrate electroreduction: mechanism insight, in situ characterization, performance evaluation, and challenges. *Chem. Soc. Rev.* **2021**, *50*, 6720−6733.
(126) Wei, L.; Liu, D.-J.; Rosales, B. A.; Evans, J. W.; Vela, J. Mild and Selective Hydrogenation of Nitrate to Ammonia in the Absence of Noble Metals. *ACS Catal.* **2020**, *10*, 3618−3628.
(127) Xu, P.; Agarwal, S.; Lefferts, L. Mechanism of nitrite hydrogenation over Pd/γ-Al2O3 according a rigorous kinetic study. *J. Catal.* **2020**, *383*, 124−134.
(128) Zhu, I.; Getting, T. A review of nitrate reduction using inorganic materials. *Environ. Technol. Rev.* **2012**, *1*, 46−58.
(129) Bowers, C. R.; Weitekamp, D. P. Para-Hydrogen And Synthesis Allow Dramatically Enhanced Nuclear Alignment. *J. Am. Chem. Soc.* **1987**, *109* (18), 5541−5542.

https://doi.org/10.1021/jacs.2c02619
J. Am. Chem. Soc. 2022, 144, 8756−8769